Spectroscopic Investigation of Peroxide Binding to the Trinuclear Copper Cluster Site in Laccase: Correlation with the Peroxy-Level Intermediate and Relevance to Catalysis

Uma M. Sundaram,[†] Hua H. Zhang,[†] Britt Hedman,[‡] Keith O. Hodgson,[†,‡] and Edward I. Solomon*,[†]

Contribution from the Department of Chemistry, Stanford University, and Stanford Synchrotron Radiation Laboratory, Stanford, California 94305

Received June 20, 1997[⊗]

Abstract: Laccase is a multicopper oxidase which contains four coppers, one type 1, one type 2, and a coupled binuclear type 3 pair, the type 2 and type 3 copper centers together forming a trinuclear copper cluster. The type 1 mercury derivative of laccase (T1Hg Lc) has the type 1 center substituted with a redox-inactive Hg^{2+} ion and an intact trinuclear copper cluster. Reaction of H_2O_2 with fully oxidized T1Hg Lc produces a peroxide adduct which has now been studied in detail. Peroxide is shown to bind to the trinuclear cluster with low affinity, producing spectral and geometric features similar to the intermediate formed in the reduction of O_2 to H_2O which had been shown to have the type 2 copper reduced, the type 3 pair oxidized and antiferromagnetically coupled, and two coppers bridged at a distance of 3.4 Å. The peroxide adduct and the intermediate have similar geometric and electronic features with the type 2 oxidized in the adduct. This center is paramagnetic and has been studied in detail. Peroxide binds to the type 2 center. EPR and ligand field (NiR MCD) coupled with CT (absorption and MCD) data demonstrate that peroxide binds to the type 2 Cu which goes from being 3-coordinate in the resting protein to 4-coordinate in the peroxide adduct. Peroxide also binds to the type 3 site from a comparison of ligand field absorption and CD and the presence of more than one intense $O_2^{2-} \rightarrow$ Cu(II) band in the CT absorption spectrum. A bridging interaction between coppers at 3.4 Å is seen from the EXAFS data. Possible geometric structures for the peroxide adduct and intermediate are proposed, with the electronic structural difference between the adduct and the intermediate being related to the type 2 copper being reduced in the latter. This study (i) firmly establishes the role of the type 2 in catalysis, (ii) demonstrates a type 2/type 3 bridging mode of binding that promote further $2e^-$ reduction of peroxide to water, and (iii) provides further support for a peroxide-level intermediate in the catalytic cycle of the multicopper oxidases which involve two $2e^-$ steps in the reduction of O_2 to H_2O.

Introduction

Laccase (Lc), ascorbate oxidase (AO), and ceruloplasmin are the known multicopper oxidases which catalyze the 4-electron reduction of dioxygen to water.[1−6] Laccase[6] (*p*-diphenol: dioxygen oxidoreductase, EC 1.10.3.2) is the simplest of the multicopper oxidases containing a total of four copper centers which are divided into three types: type 1, a blue copper center with characteristic spectral features (an intense absorption band at ∼600 nm ($\epsilon \sim 5000\ M^{-1}\ cm^{-1}$) and a small parallel hyperfine coupling ($A_{\|} \sim 40-70 \times 10^{-4}\ cm^{-1}$) in the electron paramagnetic resonance (EPR) spectrum); type 2, a mononuclear copper center with normal spectral features; and type 3, a binuclear copper site where the coppers are antiferromagnetically coupled through a bridging ligand, hence EPR silent.[7−10] Ascorbate oxidase[5,11,12] can be described as a dimer of laccase sites with a total of eight coppers, while ceruloplasmin[3,6] contains three type 1,[13] one type 2, and one type 3 center. Antiferromagnetically coupled binuclear copper sites are also present in hemocyanin and tyrosinase,[14,15] which reversibly bind and activate dioxygen, respectively.

Spectroscopy combined with crystallography has generated a detailed description of the active site in laccase and ascorbate oxidase. Magnetic circular dichroism (MCD)[10,16,17] and X-ray absorption spectroscopy[18] on laccase have shown that the type

* To whom all correspondence should be addressed.
[†] Department of Chemistry, Stanford University.
[‡] Stanford Synchrotron Radiation Laboratory.
[⊗] Abstract published in *Advance ACS Abstracts,* November 15, 1997.

(1) Malkin, R.; Malmström, B. G. *Adv. Enzymol. Relat. Areas Mol. Biol.* **1970**, *33*, 177.
(2) Malmström, B. G.; Andréasson, L.-E.; Reinhammar, B. In *Enzymes*, 3rd ed.; Boyer, P. D., Ed.; Academic: New York, 1975; Vol. 12, p 507.
(3) Ryden, L. In *Copper Proteins and Copper Enzymes*; Lontie, R., Ed.; CRC Press: Boca Raton, FL, 1984; Vol. III, p 37.
(4) Solomon, E. I.; Lowery, M. D. *Science* **1993**, *259*, 1575.
(5) Messerschmidt, A. *Perspectives in Bioinorganic Chemistry* **1996**, *3*, 151.
(6) Solomon, E. I.; Sundaram, U. M.; Machonkin, T. E. *Chem. Rev.* **1996**, *96*, 2563.
(7) Solomon, E. I.; Dooley, D. M.; Wang, R. H.; Gray, H. B.; Cerdonio, M.; Mogno, F.; Romani, G. L. *J. Am. Chem. Soc.* **1976**, *98*, 1029.
(8) Petersson, L.; Ångstrom, J.; Ehrenberg, A. *Biochim. Biophys. Acta* **1978**, *526*, 311.
(9) Dooley, D. M.; Scott, R. A.; Ellinghaus, J.; Solomon, E. I.; Gray, H. B. *Proc. Natl. Acad. Sci. U.S.A.* **1978**, *75*, 3019.
(10) Cole, J. L.; Clark, P. A.; Solomon, E. I. *J. Am. Chem. Soc.* **1990**, *112*, 9534.
(11) Mondoví, B.; Avigliano, L. In *Copper Proteins and Copper Enzymes*; Lontie, R., Ed.; CRC Press, Inc.: Boca Raton, FL, 1984; Vol. III, p 101.
(12) Messerschmidt, A.; Rossi, A.; Ladenstein, R.; Huber, R.; Bolognesi, M.; Guiseppina, G.; Marchesini, A.; Petruzzelli, R.; Finazzi-Agro, A. *J. Mol. Biol.* **1989**, *206*, 513.
(13) Machonkin, T. E.; Solomon, E. I.; et al. To be published.
(14) Solomon, E. I.; Baldwin, M. J.; Lowery, M. D. *Chem. Rev.* **1992**, *92*, 521.
(15) Magnus, K. A.; Ton-That, H.; Carpenter, J. E. In *Bioinorganic Chemistry of Copper*; Karlin, K. D., Tyeklar, Z., Eds.; Chapman & Hall: New York, 1993; p 143.
(16) Allendorf, M. D.; Spira, D. J.; Solomon, E. I. *Proc. Natl. Acad. Sci. U.S.A.* **1985**, *82*, 3063.
(17) Spira-Solomon, D. J.; Allendorf, M. D.; Solomon, E. I. *J. Am. Chem. Soc.* **1986**, *108*, 5318.
(18) Cole, J. L.; Tan, G. O.; Yang, E. K.; Hodgson, K. O.; Solomon, E. I. *J. Am. Chem. Soc.* **1990**, *112*, 2243.

S0002-7863(97)02039-8 CCC: $14.00

2 and type 3 centers combine to function as a trinuclear copper cluster with respect to exogenous ligand interactions including reaction with dioxygen. Crystallography[12,19,20] also shows a trinuclear copper cluster in ascorbate oxidase and ceruloplasmin. The type 2 center is 3-coordinate with two histidines and a water as ligands. The type 3 coppers are each 4-coordinate, having three histidine ligands and a bridging hydroxide. All coppers of the type 2/type 3 trinuclear copper cluster are within 3.8 Å of each other. The type 1 blue copper site is approximately 12.5 Å away from the trinuclear cluster but connected to it by a type 1−Cys-His−type 3 pathway for electron transfer. In the crystal structure of the fully reduced enzyme,[21] the coordination environments of the type 1 and type 2 centers are unchanged while the hydroxide bridge at the type 3 site is lost. The separation between the two type 3 coppers increases to 5.1 Å. A structure for the peroxide adduct of fully oxidized ascorbate oxidase has also been reported (*vide infra*).[21]

The reaction of fully reduced (i.e., 4-electron) laccase with O_2 has been studied in some detail, and a number of mechanisms have been proposed.[21−23] There is one intermediate observed in the reaction of the reduced native enzyme with dioxygen, which shows an $S = {}^1/_2$ EPR signal which broadens with $^{17}O_2$.[24−26] It had been thought to be a 3-electron reduced oxygen radical with the electrons contributed by the type 1 and the two type 3 coppers which are oxidized in the native intermediate, while the type 2 Cu was thought to be reduced on the basis of the lack of its EPR signal. However, MCD studies[27] have shown that the $S = {}^1/_2$ center in the native intermediate has significant Cu(II) character, leading to an alternative description of the native intermediate as a 4-electron reduced hydroxide product bound to a fully oxidized trinuclear cupric site. Two derivatives of laccase have been useful in defining the metal center requirements for oxygen reduction. The type 2 depleted (T2D) derivative[28] has the type 2 center reversibly removed and thus contains only the type 1 and the type 3 centers. Reduced T2D laccase does not react with dioxygen,[18] demonstrating the requirement of the type 2 center for oxygen reduction. A second derivative, T1Hg Lc,[29] has the type 1 center replaced by a redox inactive Hg^{2+} ion but still contains an intact type 2/type 3 trinuclear copper cluster site.[30] The fully reduced (i.e., 3-electron) T1Hg Lc derivative reacts with dioxygen, showing that the type 2/type 3 trinuclear copper cluster is the minimum structural unit for dioxygen reduction.[18]

The type 1 center in the T1Hg Lc derivative is no longer capable of transferring an electron to dioxygen reacting at the trinuclear copper site. This enables a new oxygen intermediate to be generated[31] which is at least one electron less reduced than the native intermediate. The rate of formation of the T1Hg Lc oxygen intermediate is the same as that of the oxygen intermediate of native Lc 10^6 M^{-1} s^{-1},[31] indicating that the T1Hg Lc oxygen intermediate is kinetically competent to be the precursor to the native Lc oxygen intermediate. Detailed spectroscopic studies on the T1Hg Lc oxygen intermediate[32] revealed that it is a peroxide-level intermediate in which both oxygen atoms are bound, two electrons are transferred from the type 3 site, and the type 2 copper is reduced. This intermediate is diamagnetic with a Cu···Cu bridging interaction at 3.4 Å. A spectroscopically effective model for this intermediate was proposed in which the peroxide is bound as hydroperoxide bridging between the type 2 and type 3 sites in a μ-1,1 mode.[32] The assignment of a peroxide-level intermediate in the catalytic cycle, prompted us to pursue the study of peroxide binding to a fully oxidized trinuclear cluster in the T1Hg Lc derivative. This form has the advantage of having an oxidized type 2 center, permitting detailed spectral studies of the interaction of peroxide with this site. Earlier reports have suggested a high-affinity binding of peroxide to native laccase (10^8 M^{-1})[33] and T2D laccase (10^4 M^{-1}),[34] which have in fact been shown to be oxidation of the type 3 site.[35,36] In this study, H_2O_2 is found to bind with low affinity (10^1 M^{-1}) to the oxidized trinuclear site. It binds in a manner similar to that of the intermediate, with a Cu···Cu bridging interaction at 3.4 Å as seen from the EXAFS (extended X-ray absorption fine structure) data.[32] We have used spectral data to construct structural models for peroxide bound to the trinuclear cluster. This geometric and electronic structure description provides insight into the function which is to promote further reduction of peroxide to water and into the role of the different coppers at the trinuclear cluster in oxygen binding.

Experimental Section

Rhus vernicifera laccase was isolated[37,38] from the acetone powder (Saito and Co., Osaka, Japan). Laccase activity was assayed spectrophotometrically using *N*,*N*-dimethyl-*p*-phenylenediamine as a substrate.[37] The T1Hg derivative of laccase was prepared using a hollow fiber dialysis unit (Spectrum Medical Instruments, Los Angeles, CA) according to published procedures.[29,39,40] The concentration of T1Hg Lc was measured using the absorption band at 280 nm ($\epsilon_{280} = 90\,000$ M^{-1} cm^{-1});[41] for all ligand additions, concentrations were normalized to copper concentration. The type 2 depleted (T2D) laccase was prepared according to the procedure of Graziani et al.[28] with modifications.[42] Copper concentrations were determined spectrophotometrically by the method of Felsenfeld using 2,2′-biquinoline[43] or by atomic absorption spectroscopy. All experiments were performed in 100 mM potassium phosphate buffer, pH = 6 (pD = 5.6 for SQUID magnetic susceptibility), at room temperature unless otherwise specified. Per-

(19) Messerschmidt, A.; Ladenstein, R.; Huber, R.; Bolognesi, M.; Avigliano, L.; Petruzzelli, R.; Rossi, A.; Finazzi-Agrò, A. *J. Mol. Biol.* **1992**, *224*, 179.
(20) Zaitseva, I.; Zaitsev, V.; Card, G.; Moshov, K.; Bax, B.; Ralph, A.; Lindley, P. *J. Biol. Inorg. Chem.* **1996**, *1*, 15.
(21) Messerschmidt, A.; Luecke, H.; Huber, R. *J. Mol. Biol.* **1993**, *230*, 997.
(22) Reinhammar, B. In *Copper Proteins and Copper Enzymes*; Lontie, R., Ed.; CRC Press: Boca Raton, FL, 1984; Vol. III, p 1.
(23) Farver, O. In *Gas Enzymology, Proceedings Symposium 1985, Meeting Date 1984*; Degn, H., Cox, R. P., Toftlund, H., Eds.; Reidel: Dordrecht, The Netherlands, 1985; p 61.
(24) Deinum, J.; Vänngård, T. *FEBS Lett.* **1975**, *58*, 62.
(25) Aasa, R.; Brändén, R.; Deinum, J.; Malmström, B. G.; Reinhammar, B.; Vänngård, T. *Biochem. Biophys. Res. Commun.* **1976**, *70*, 1204.
(26) Brändén, R.; Deinum, J. *FEBS Lett.* **1977**, *73*, 144.
(27) Clark, P. A.; Solomon, E. I. *J. Am. Chem. Soc.* **1992**, *114*, 1108.
(28) Graziani, M. T.; Morpurgo, L.; Rotilio, G.; Mondoví, B. *FEBS Lett.* **1976**, *70*, 87.
(29) Morie-Bebel, M. M.; Morris, M. C.; Menzie, J. L.; McMillin, D. R. *J. Am. Chem. Soc.* **1984**, *106*, 3677.
(30) Klemens, A. S.; McMillin, D. R.; Tsang, H. T.; Penner-Hahn, J. E. *J. Am. Chem. Soc.* **1989**, *111*, 6398.
(31) Cole, J. L.; Ballou, D. P.; Solomon, E. I. *J. Am. Chem. Soc.* **1991**, *113*, 8544.
(32) Shin, W.; Sundaram, U. M.; Cole, J. L.; Zhang, H. H.; Hedman, B.; Hodgson, K. O.; Solomon, E. I. *J. Am. Chem. Soc.* **1996**, *118*, 3202.
(33) Farver, O.; Goldberg, M.; Lancet, D.; Pecht, I. *Biochem. Biophys. Res. Commun.* **1976**, *73*, 494.
(34) Farver, O.; Frank, P.; Pecht, I. *Biochem. Biophys. Res. Commun.* **1982**, *108*, 273.
(35) Kau, L.-S.; Spira-Solomon, D. J.; Penner-Hahn, J. E.; Hodgson, K. O.; Solomon, E. I. *J. Am. Chem. Soc.* **1987**, *109*, 6433.
(36) Hahn, J. E.; Co, M. S.; Spira, D. J.; Hodgson, K. O.; Solomon, E. I. *Biochem. Biophys. Res. Commun.* **1983**, *112*, 737.
(37) Reinhammar, B. *Biochim. Biophys. Acta* **1970**, *205*, 35.
(38) Reinhammar, B. *Biochim. Biophys. Acta* **1972**, *275*, 245.
(39) Severns, J. C.; McMillin, D. R. *Biochemistry* **1990**, *29*, 8592.
(40) Morie-Bebel, M. M.; Menzie, J. L.; McMillin, D. R. In *Biol. Inorg. Copper Chemistry, Proceedings of Conference on Copper Coordination Chemistry, 2nd, Meeting Date 1984*; Karlin, K. D., Zubieta, J., Eds.; Adenine Press: Guilderland, NY, 1986; Vol. 1, p 89.
(41) Meadows, K. A.; Morie-Bebel, M. M.; McMillin, D. R. *J. Inorg. Biochem.* **1991**, *41*, 253.
(42) Klemens, A. S.; McMillin, D. R. *J. Inorg. Biochem.* **1990**, *38*, 107.
(43) Felsenfeld, G. *Arch. Biochem. Biophys.* **1960**, *87*, 247.

oxide adduct samples were prepared by adding the appropriate amount of hydrogen peroxide (30% Stock solution, Mallinckrodt) and stirring for 5−10 min. Fluoride adduct (one-fluoride-bound) samples were prepared by adding 5−10 μL of concentrated aqueous solutions to the protein and stirring for 24 h prior to the spectroscopic measurements. For low-temperature (LT) absorption, MCD, and EXAFS studies, the samples were prepared in 50% glycerol (v/v) which was required to make good-quality low-temperature glasses. Protein sample concentrations were ∼0.5 mM for absorption, EPR, CD, and MCD experiments. Slightly higher concentrations in the range ∼1.5−1.7 mM were used for SQUID magnetic susceptibility and EXAFS experiments. The concentration of H_2O_2 was measured using the absorption at 240 nm ($\epsilon_{240} = 45.6\ M^{-1}\ cm^{-1}$). Ethyl hydroperoxide was obtained as a 10% solution from Polysciences Inc. (Warrington, PA) and *tert*-butyl hydroperoxide as a 90% solution from Aldrich. All T1Hg Lc spectra were corrected for a residual amount of native laccase (estimated from activity measurements), and the peroxide adduct spectra were additionally corrected for contribution from unreacted resting T1Hg Lc protein, this amount estimated from the equilibrium binding constant and the specific protein concentration in that experiment. All chemicals were reagent grade and were used without further purification. Water was purified to a resistivity of 15−18 MΩ cm using a Barnstead Nanopure deionizing system.

UV/visible absorption spectra were recorded on a Hewlett-Packard HP8452A diode array spectrophotometer in either 10, 2, or 1 mm quartz cuvettes. Low-temperature ligand field absorption data were collected on a Cary-17 spectrophotometer using a Janis Research Super Varitemp cryogenic dewar mounted in the optical path. CD spectra were recorded using 10 or 2 mm quartz cuvettes. MCD data were obtained using a sample cell consisting of two quartz disks with a 3 mm rubber spacer. CD and MCD spectroscopy were performed with a Jasco J-500-C spectropolarimeter operating with S-1 and S-20 photomultiplier tubes for the 1050−800 and 800−300 nm regions, respectively, and a Jasco J-200-D spectropolarimeter interfaced to a Macintosh IIvx computer and a liquid nitrogen cooled InSb detector for the 600−2000 nm region. Data acquisition was achieved using routines written within the software package LabVIEW (National Instruments). Contributions to the CD intensity due to buffer and cell backgrounds were subtracted from the raw protein CD spectra. Low-temperature UV−vis, near-IR MCD spectroscopic studies utilized an Oxford Spectromag 4, SM4/7 T, or SM 4000/7 T superconducting magnetooptical dewars. The possibility of strain-induced depolarization of light by the sample glass was evaluated by a comparison of the CD spectra of a solution of nickel(+) tartrate placed before and after the sample; depolarizations of <10% were routinely obtained. Sample temperatures were measured with a carbon glass resistor (Cryogenic Calibrations, Pitchcott, Aylesbury, Buckinghamshire, U.K.). MCD spectra were corrected for zero-field baseline effects induced by cracks in the glasses by subtracting the corresponding 0 T scan at that temperature. CD and MCD spectra were smoothed using a weighted fitting routine and Gaussian resolution of absorption, CD and MCD spectra were performed using a constrained nonlinear least-squares fitting protocol. MCD intensity is reported in units of $M^{-1}\ cm^{-1}\ T^{-1}$.

EPR spectra were obtained with a Bruker ER 220-D-SRC spectrometer. Sample temperatures of 77 K were maintained using a liquid N_2 finger dewar, and temperatures from 70 to 4 K were obtained using an Air Products model LTR Helitran liquid helium transfer refrigerator and a Lake Shore Cryotronics temperature controller model DTC-500. The EPR data were spin quantitated against a Cu standard, $Cu(ClO_4)_2$ (1.0 mM $CuSO_4 \cdot 5H_2O$ with 2 mM HCl and 2 M $NaClO_4$[44]). Spectra Calc, Collect Arithmetic C2.20 from Galactic Industries Corp was used for spin integration of the EPR signals. EPR spectral simulations were performed using the QPOW computer program (obtained from Quantum Chemistry Program Exchange).

Magnetic susceptibility data were taken on a Quantum Design Model MPMS SQUID magnetometer. Mercury tetrathiocyanatocobaltate(II) and a palladium cylinder were employed as dual magnetometer calibrants. Polycarbonate capsules (Universal Plastics and Engineering Co., Rockville, Maryland) were used as sample buckets. The two halves of the capsule were sealed by applying a drop of acetone, and the cap had a hole to allow the space above the sample to be evacuated in the antechamber, prior to sample loading. The antechamber was flushed with He gas prior to sample loading. Samples were loaded frozen onto a phenolic guide (clear soda straw) which was fixed to the end of a magnetometer drive rod and loaded into the SQUID magnetometer. Sample volumes were typically 150 μL. The susceptibility vs $1/T$ data were taken in the 10−80 K temperature region at 4.0 T and fitted using a linear least-squares procedure.

X-ray absorption data for the peroxide and fluoride adducts of T1Hg Lc samples were recorded at the Stanford Synchrotron Radiation Laboratory (SSRL) on unfocused beamline 7-3 under dedicated conditions (3.0 GeV, 60−100 mA). Monochromatic radiation was obtained using a Si (220) double-crystal monochromator which was detuned 50% for harmonic rejection. The beam height was defined to be 1 mm. The fluorescence signals were measured with an Ar-filled ionization chamber detector[45,46] equipped with Soller slits and a Ni filter. Internal energy calibration was performed assigning the first inflection point of the Cu foil spectrum to be 8980.3 eV. The samples were loaded into 2 mm thick Lucite XAS cells with 63.5 μM Mylar windows, frozen immediately, and kept under liquid nitrogen prior to the measurements. The samples were maintained at a constant temperature of 10 K throughout the measurements by an Oxford Instruments CF1208 continuous-flow liquid helium cryostat.

During the measurements, both the peroxide and fluoride adduct samples showed signs of photoreduction, as seen from a gradual increase in intensity of the preedge feature at 8984 eV.[35] Thus, data were collected from two spots on each sample and the edge analysis showed ∼8% photoreduction from the first to the last scan. Comparison of all the EXAFS scans, however, did not reveal any change in the EXAFS region of the data. Therefore, all the good scans were averaged for EXAFS analysis. The data analyzed represent an average of 17−20 scans for each sample.

All of the data were processed using standard procedures for preedge subtraction, spline fit and removal, and normalization.[47−49] A nonlinear least-squares curve-fitting method using empirical phase and amplitude parameters was performed, in which the following models were used to obtain these parameters: Cu−O from Cu(acetylacetonate)$_2$,[50] Cu−N from Cu(imidazole)$_4$(NO$_3$)$_2$,[51] and Cu···Cu from [Cu(HB(3,5-*i*-Pr$_2$-pz)$_3$)]$_2$(OH)$_2$.[52] Fourier transforms (FTs) were calculated over the data range 3.5−12.5 Å^{-1} with a Gaussian window of 0.1 Å^{-1} and were then back-transformed with a Fourier filtering window centered on the peak of interest (see Results and Analysis). All curve-fitting was performed with k^3-weighted data by varying the structure-dependent parameters, i.e. the distance and Debye−Waller (DW) factor with fixed coordination number (CN) or distance and variable CN with fixed DW factor. A goodness-of-fit value, F, was calculated as $F = \{[k^6(\text{data} - \text{fit})^2]/(\text{no. of points})\}^{1/2}$ for each fit and used for evaluation of the fit results.

Results and Analysis

I. Low-Affinity Peroxide Binding. (a) Figure 1A,B presents a titration of T1Hg Lc with increasing concentrations of H_2O_2 as monitored by optical absorption spectroscopy in the 300−820 nm region. Shown in Figure 1A are the titration spectra and in Figure 1B the difference absorption spectra obtained by subtraction of resting untreated T1Hg Lc protein spectrum from those in Figure 1A. Figure 1C shows a similar titration experiment monitored by EPR at 77 K. The absorption

(44) Carithers, R. P.; Palmer, G. *J. Biol. Chem.* **1981**, *256*, 7967.
(45) Stern, E. A.; Heald, S. M. *Rev. Sci. Instrum.* **1979**, *50*, 1579.
(46) Lytle, F. W.; Greegor, R. B.; Sandstrom, E. R.; Marques, E. C.; Wong, J.; Spiro, C. L.; Huffman, G. P.; Huggins, R. E. *Nucl. Instrum. Methods* **1984**, *226*, 542.
(47) Cramer, S. P.; Hodgson, K. O.; Stiefel, E. I.; Newton, W. E. *J. Am. Chem. Soc.* **1978**, *100*, 2748.
(48) Cramer, S. P.; Hodgson, K. O. *Prog. Inorg. Chem.* **1979**, *15*, 1.
(49) Scott, R. A. *Methods Enzymol.* **1985**, *117*, 414.
(50) Starikova, Z. A.; Shugam, E. A. *Zh. Struckt. Khim.* **1969**, *10*, 290.
(51) McFadden, D. L.; McPhail, A. T.; Garner, C. D.; Mabbs, F. E. *J. Chem. Soc., Dalton Trans.* **1976**, 47.
(52) Kitajima, N.; Fujisawa, K.; Fujimoto, C.; Moro-oka, Y.; Hashimoto, S.; Kitagawa, T.; Toriumi, K.; Tatsumi, K.; Nakamura, A. *J. Am. Chem. Soc.* **1992**, *114*, 1277.

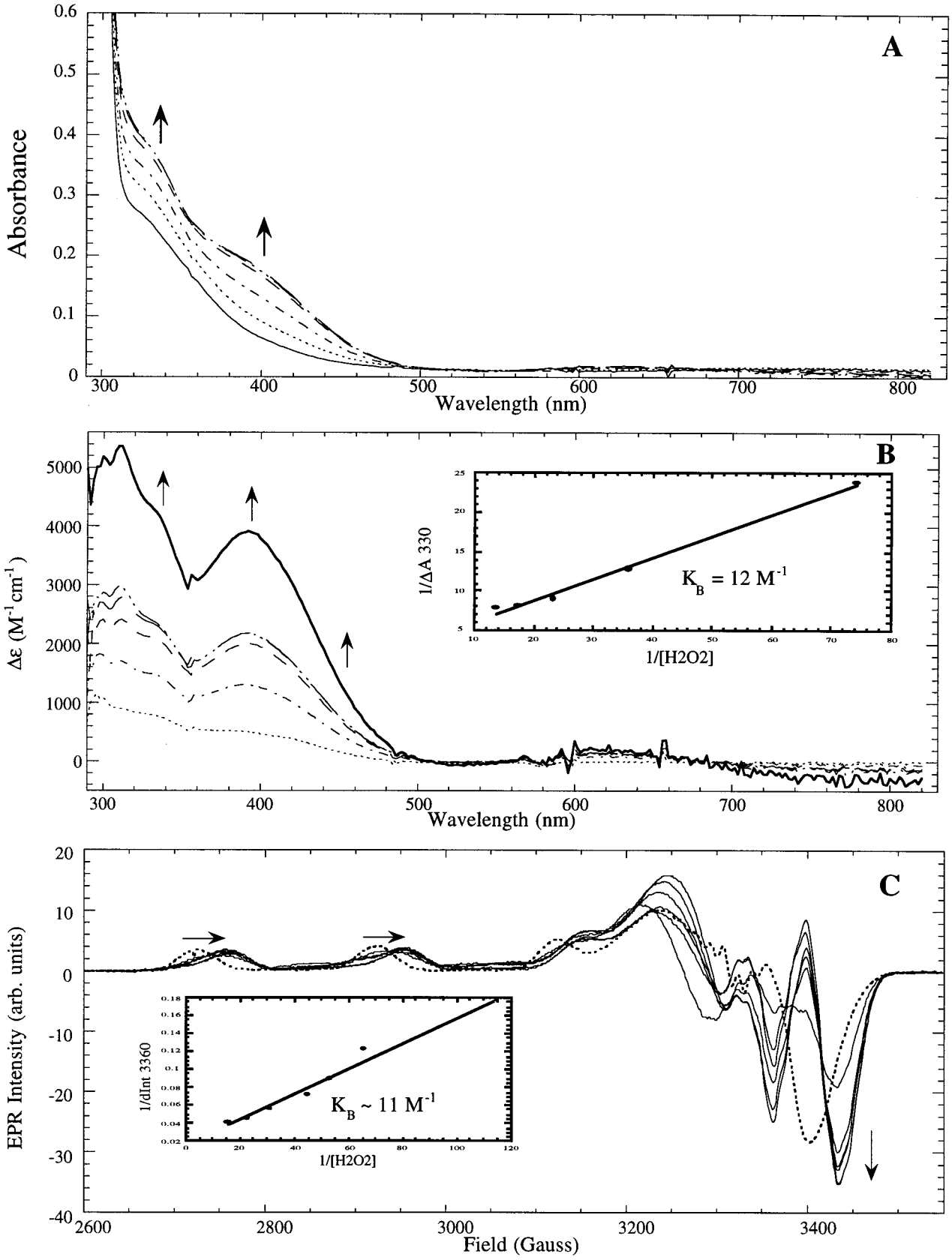

Figure 1. (A) Room-temperature absorption titration of T1Hg Lc with increasing concentrations of H_2O_2: (—) resting, (- - -) 50, (- · -) 100, (— — —) 150, (— - —) 200, and (— ··· —) 250 mol excess per mole of protein. (B) Difference absorption spectra of A (bound, resting untreated protein). The thick solid line is fully converted adduct (see text). The inset shows a Scatchard plot which gives a binding constant K_B of 12 M^{-1}. (C) 77 K X-band EPR titration of T1Hg Lc with increasing concentrations of H_2O_2: 30, 60, 100, 150, 200, and 300 mol per mole of protein. Resting untreated T1Hg Lc is the dotted spectrum, and the solid lines are the titration spectra. A Scatchard plot (inset) of the feature growing in at 3360 G as a function of H_2O_2 concentration gives a K_B of 11 M^{-1}. Arrows indicate the changes with increasing $[H_2O_2]$.

difference spectra clearly exhibit bands at 338 nm ($\epsilon \sim 4000$ M^{-1} cm^{-1}) and 392 nm ($\epsilon \sim 3800$ M^{-1} cm^{-1}) as indicated by arrows (and weaker low-energy bands at ~430 nm ($\epsilon \sim 1300$ M^{-1} cm^{-1}) and 460 nm ($\epsilon \sim 600$ M^{-1} cm^{-1}) *vide infra*), which

increase in intensity with increasing peroxide concentration, indicating that these bands are associated with peroxide binding. The thick solid trace in Figure 1B is the difference absorption spectrum of the fully converted adduct from which the unbound T1Hg Lc has been subtracted and the resultant spectrum renormalized. The percentage unbound is based on equilibrium binding constant (*vide infra*) and the specific protein concentration. Significant and systematic changes also occur in the EPR titration, with a shift of the $M_I = -^3/_2$ type 2 hyperfine line to higher field with concomitant growth of a feature at 3360 G in the perpendicular region (arrows in Figure 1C). These changes increase with increasing concentrations of H_2O_2, indicating that these are associated with peroxide binding. These changes in the absorption and EPR spectra are plotted as a function of H_2O_2 concentration to obtain equilibrium binding constants. Scatchard plots (insets in the figure (1B and 1C)) give a peroxide binding constant (K_B) to T1Hg Lc of 12 ($\pm$4) M^{-1}. H_2O_2 thus binds with a low affinity to the fully oxidized trinuclear Cu cluster. This low-affinity H_2O_2 binding is not to be confused with early reports of peroxide binding with high affinity ($K_B > 10^8$ M^{-1})[33] which corresponds to oxidation of ~23% reduced type 3[53] centers (present in as-isolated native laccase).

The 10 K absorption spectrum of the peroxide adduct shows identical features to those at room temperature (see the Supporting Information). Thus, spectroscopic data obtained at low temperatures can be compared with room-temperature results and with physiologically relevant enzymological events. An absorption titration at room temperature was performed in the presence of 50% (v/v) glycerol; the spectral changes and binding constant (K_B) were identical with those in the absence of glycerol. Therefore glycerol also has no affect on binding of H_2O_2 at the active site. Peroxide binding was investigated by absorption, EPR, and MCD spectroscopies in the pH range 5 (0.1 M, MES) to 8 (0.1 M, HEPES). No change was observed in binding affinity or in spectral features over this pH range. Binding of alkyl peroxides (ethyl hydroperoxide and *tert*-butyl hydroperoxide) was probed using absorption and EPR spectroscopies. At very high ligand excesses, the absorption spectra showed very minor spectral changes and the EPR spectra showed no changes, suggesting lack of binding of the alkyl peroxides. This lack of observable binding could be either due to difficulty of access to the site by the bulkier alkyl peroxides or due to inability to bind in a preferred mode due to the presence of the R group instead of the proton.

(b) H_2O_2 binding to native laccase was probed by absorption and EPR spectroscopies (see the Supporting Information). The spectral changes were identical with those obtained with T1Hg Lc, indicating that a low-affinity binding of H_2O_2, which parallels that in T1Hg Lc, occurs in the catalytically relevant native laccase enzyme.

(c) H_2O_2 was added to the type 3 oxidized T2D derivative (met-T2D)[54,55] in increasing amounts up to 250-fold excess and investigated by absorption, EPR, and CD spectroscopies (see the Supporting Information). No perceptible change in any of the spectra was observed on H_2O_2 addition. Binding of the peroxide ligand to the type 3 oxidized (met) T2D is not observed. From the lack of changes in the spectral features with 250-fold excess of peroxide, an upper limit of K_B of < 1 M^{-1} is obtained, which is at least 1 order of magnitude lower than that of O_2^{2-} binding to the trinuclear cluster. This result indicates that the type 2 copper is required for the binding of H_2O_2.

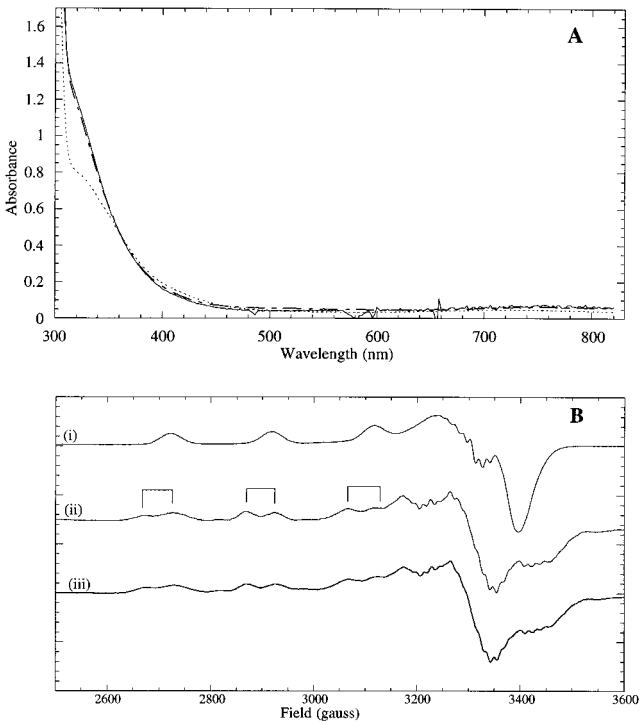

Figure 2. (A) Room-temperature absorption spectra of (- - -) resting T1Hg Lc, (− - −) T1Hg Lc + 1 equiv of F^-, (—) T1Hg Lc + 1 equiv of F^- + 200-fold excess H_2O_2. (B) 77 K X-band EPR spectra of (i) resting T1Hg Lc, (ii) T1Hg Lc + 1 equiv of F^- (the F^- superhyperfine splitting on the Cu hyperfine are indicated), and (iii) T1Hg Lc + 1 equiv of F^- + 200-fold excess H_2O_2.

(d) F^- binds to the type 2 copper with a high binding constant[17,56] and depending upon the conditions one or two F^-'s bind, to produce a doublet (1F) or triplet (2F) F^- superhyperfine splitting superimposed on each Cu hyperfine feature in the EPR spectrum.[10] Figure 2A,B shows the effect of one fluoride binding by absorption (growth of a CT band at ~320 nm) and EPR spectra, respectively. The large superhyperfine associated with the F^- binding requires equatorial binding to the type 2 site,[10,17] which likely occurs by addition to the open coordination position of the type 2 site (*vide infra*). A 200-fold excess H_2O_2 was added to the one-fluoride-bound form of T1Hg Lc, and its absorption and EPR spectra were recorded (Figure 2A (solid line) and Figure 2B(iii)). From Figure 2, there is no change in either the absorption or EPR spectra on peroxide addition, indicating that H_2O_2 does not bind to the one-fluoride-bound form of the enzyme. Inhibition of H_2O_2 binding, by F^- bound at the type 2 site, also indicates that H_2O_2 likely coordinates to the type 2 site.

(e) Reversibility of peroxide binding: The peroxide ligand may be removed either by dialysis or by allowing the peroxide to decay over time. In both cases, the absorption, EPR, and MCD spectral changes caused by the peroxide addition are completely reversed. This demonstrates that the spectral changes observed are not due to irreversible damage of the protein by peroxide and indicates that the peroxide ligand likely binds with its O−O bond intact, rather than forming a binuclear

(53) Penner-Hahn, J. E.; Hedman, B.; Hodgson, K. O.; Spira, D. J.; Solomon, E. I. *Biochem. Biophys. Res. Commun.* **1984**, *119*, 567.

(54) The type 3 oxidized T2D derivative (met-T2D) was prepared by addition of 30-fold excess H_2O_2 to the reduced type 3 T2D (deoxy T2D) derivative followed by dialysis.

(55) LuBien, C. D.; Winkler, M. E.; Thamann, T. J.; Scott, R. A.; Co, M. S.; Hodgson, K. O.; Solomon, E. I. *J. Am. Chem. Soc.* **1981**, *103*, 7014.

(56) Brändén, R.; Malmström, B. G.; Vänngård, T. *Eur. J. Biochem.* **1973**, *36*, 195.

(57) Mahapatra, S.; Halfen, J. A.; Wilkinson, E. C.; Pan, G.; Wang, X.; Young, V. G.; Cramer, C. J.; Que, L.; Tolman, W. B. *J. Am. Chem. Soc.* **1996**, *118*, 11555.

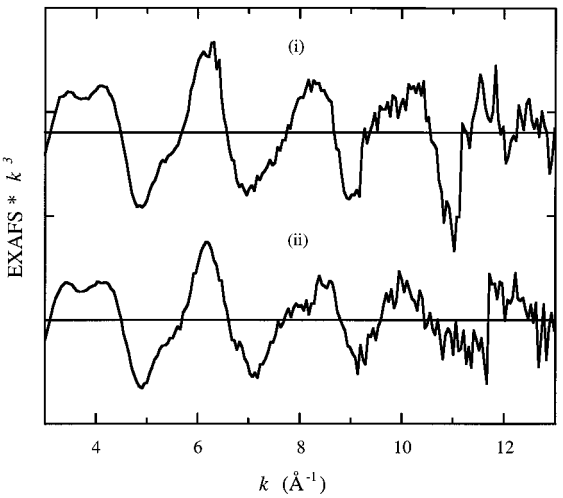

Figure 3. EXAFS spectra of (i) peroxide adduct and (ii) fluoride adduct of T1Hg laccase. (The ordinate scale is 5 between two consecutive tick marks.)

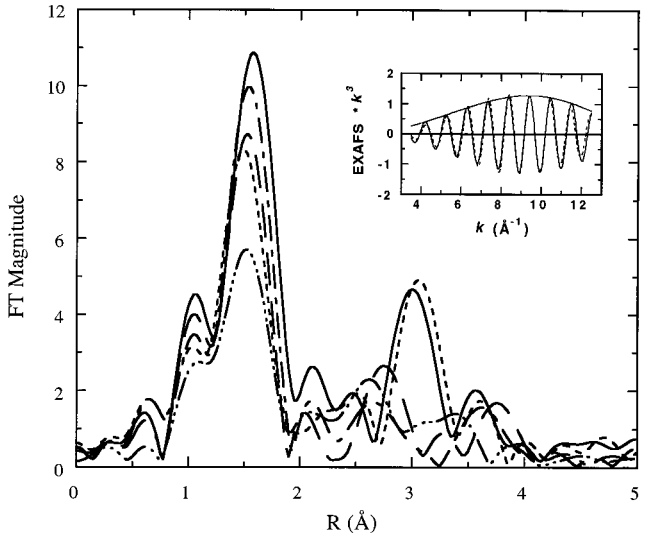

Figure 4. Non-phase-shift-corrected Fourier transforms of the EXAFS data for the (—) peroxide adduct, (– - –) oxidized, (– – –) fluoride adduct, (- - -) intermediate, and (– ··· –) reduced T1Hg laccase. The significant difference among the five is the presence of a 3.0 Å peak in the FT data of peroxide adduct and intermediate of T1Hg laccase. The FT peak positions are offset to lower R by an atom-dependent phase shift of ~0.4 Å. Inset: Fourier back-transform of the 3.0 Å peak for the peroxide adduct of T1Hg laccase (—) and the fit (- - -) to the data.

Cu(III) bis-μ-oxo type species.[57,58] The lack of Cu(III)−oxo type species is also supported by the EXAFS data on the adduct given below.

II. EXAFS. EXAFS data were obtained from both the peroxide adduct and fluoride adduct (one-fluoride-bound form) T1Hg Lc samples to gain metrical information on these exogenous ligands bound to the trinuclear copper center. The F^- adduct form of the protein was included in this study since this ligand has been found to have a strong binding interaction with the trinuclear cluster.[10] The EXAFS spectra of the two samples are shown in Figure 3. Both spectra exhibit high-quality data out to $k = 13$ Å^{-1}. Their corresponding FTs over the k range 3.5−12.5 Å^{-1} are given in Figure 4. The FTs of the data for the reduced, oxidized, and intermediate T1Hg Lc (previously reported[32]) are also shown in Figure 4 for direct comparison. It should be noted that the FTs shown are not phase-shift corrected. The data and their analysis reflect the average contributions from all three Cu's of the trinuclear center.

(58) Mahadevan, V.; Hou, Z.; Cole, A. C.; Root, D. E.; Solomon, E. I.; Stack, T. D. P. *J. Am. Chem. Soc.*, in press.

Table 1. Summary of EXAFS Curve-Fitting Results for Peroxide Adduct of T1Hg Laccase[a]

fit no.	FT window (Å)	element	CN[b]	distance (Å)	c2[c]	F
1	0.80−1.95	N	3.0	2.00	−0.017	0.43
2	0.80−1.95	N	3.2	2.00	−0.017	0.42
3	0.80−1.95	N	4.0	2.00	−0.021	0.47
4	0.80−1.95	O	3.0	1.97	−0.019	0.40
5	0.80−1.95	O	3.2	1.97	−0.020	0.40
6	0.80−1.95	O	4.0	1.97	−0.023	0.44
7	0.80−1.95	N	2.0	2.01	−0.020	0.39
		O	1.2	1.95	−0.015	
8	0.80−1.95	N	1.2	2.00	−0.020	0.39
		O	2.0	1.96	−0.019	
9	2.65−3.32	Cu	0.67	3.35	−0.025	0.18
10	2.65−3.32	Cu	1.0	3.35	−0.029	0.17

[a] Errors are estimated to be about ±0.02 Å for distances and 25% for coordination numbers.[47−49] [b] CN = coordination number. [c] c2 is the amplitude parameter having the functional form of the DW factor, i.e., $\exp(-2\sigma^2 k^2)$, where c2 = $-2\sigma^2$. A more negative value of c2 denotes a larger value of σ^2 and thus a more disordered structure.

An inspection of the FTs in Figure 4 reveals a prominent FT peak at ~3 Å for the peroxide adduct which is absent in the data of the fluoride adduct. This peak also appears in the FT of the data for the T1Hg Lc intermediate, which shows a nearly identical peak position and intensity. A Fourier back-transform of this peak for the peroxide adduct gives rise to an EXAFS wave that is characteristic of a high-Z backscatterer, with the amplitude envelope peaking at high k (inset in Figure 4). In view of a possible Cu···Cu interaction in the trinuclear site, full-matrix least-squares curve-fitting analysis, using Cu···Cu parameters extracted from a dihydroxy-bridged binuclear Cu(II) model complex $[Cu(HB(3,5\text{-}i\text{-}Pr_2pz)_3)]_2(OH)_2$,[52] were performed by varying the distance and DW factor. The fit result gives 0.67−1 Cu at a distance of 3.35 Å (Table 1). This result is very similar to that obtained from curve fitting of the data for the intermediate T1Hg Lc.[32] The calculated DW factor is small, suggesting that the Cu···Cu interaction exists in a regular or rigid structure. The possibility of a Cu−O−Cu multiple-scattering (MS) contribution to this FT feature was tested. It was found that the MS effects were insignificant, given that the Cu···Cu and Cu−O distances (see below) result in a Cu−O−Cu angle of <130°. There is a slight mismatch between the filtered data and the fit (Figure 4 inset), which is probably due to the presence of low-Z backscatterer contributions that were not modeled in the fit.

The FT of the data for the fluoride adduct, on the other hand, lacks the peak at ~3 Å. It does, however, show a small peak at 2.7 Å. An attempt to fit this peak using a Cu backscatterer as with the peroxide adduct did not give satisfactory results. The back-transform of the peak generates an EXAFS wave that shows no clear sign of a high-Z backscatterer. The "best" fit shows a large mismatch between the data and the fit (data not shown), and the refined DW factor is nearly 50% larger than that in the peroxide adduct case. The 2.7 Å peak, however, may have significant contributions from imidazole outer-shell atoms. A comparison with the FT of the data for a Cu imidazole coordination compound strongly suggests that this is the case (data not shown). The 3.4 Å Cu···Cu bridging interaction observed in the peroxide-bound forms thus appears not to be a general feature of exogenous ligand binding at the trinuclear cluster.

The FTs and the fitting results show a strong similarity between the peroxide adduct and the intermediate T1Hg Lc,

suggesting a similar trinuclear structural model for the peroxide adduct of T1Hg Lc. The only apparent difference between the two is the intensity and position of the first-shell FT peak. The FT peak for the peroxide adduct has a higher intensity (1.1 vs 0.8) and shifts slightly toward higher *R*. The difference in intensity can be explained by comparing the FTs in Figure 4. A trend of increasing FT intensity for the first-shell peak can be seen on going from the reduced, to the intermediate, and to the oxidized T1Hg Lc, suggesting a systematic change as a result of the change in oxidation state and thus coordination of the Cu's. The fully oxidized trinuclear copper cluster in the peroxide adduct follows this trend with a higher FT intensity than present in the T1Hg Lc intermediate which is a mixture of Cu(I) and Cu(II) centers and thus is expected to have a larger spread in Cu−N/O distances.

Least-squares analysis of the data contained in the first shell of the FT of the peroxide adduct were performed to quantify the differences in this first-shell FT peak and to examine the near-neighbor environment of the copper centers in the peroxide adduct (Table 1). The fits were first performed with one single O or one single N wave, by stepping through fixed CN while varying the bond distance and the DW factor. The single-shell fitting results show that a minimum can be reached with either a Cu−N distance of 2.00 Å or a Cu−O distance of 1.97 Å and that the best fit gives a CN of 3 or 4 (with a minimum at 3.2) in both cases. Two-shell fits with one N and one O waves were also performed. The results do not show a significant improvement over the single-shell fits, and the two waves tend to converge to the same distance. Comparison of these fit results with those from the intermediate and the oxidized T1Hg Lc[32] show that the first-shell CN of both the peroxide adduct and the intermediate T1Hg Lc were refined to be between 3 and 4, with an insignificant difference of 3.2 vs 3.4. Therefore, the CN contributes little to the intensity difference of the first FT peak, and the difference is mainly due to the change in DW factor reflecting a more even coordination with higher oxidation states of the Cu's. The average first-shell distance in the peroxide adduct, however, is ∼0.03 Å longer than that in the intermediate, explaining the shift of the first FT peak in the peroxide adduct.

Curve fitting analysis was also performed in the first shell to probe for the presence of short Cu−oxo bond. However, no Cu−O distance less than 1.85 Å was found in the peroxide adduct. This observation along with the absence of an energy shift in the edge spectrum[59] of the peroxide adduct relative to the resting protein (data not shown) indicates that the O−O bond has not been cleaved to form a bis-μ-oxo $[Cu(III)]_2$ species.

III. EPR. Figure 5A,B shows the 77 K X-band EPR spectra of resting and fully converted peroxide-bound T1Hg Lc, respectively, along with their simulations. Large changes occur in the EPR spectrum of the type 2 Cu(II) center, yet both resting and peroxide-bound T1Hg Lc quantitate to 0.95 ± 0.07 spins vs an EPR standard. From the spin Hamiltonian parameters obtained from the simulations (Table 2) the *g* values of the type 2 center have changed significantly on going from the resting site to the peroxide adduct. The rhombic g_x and g_y have become axial in the adduct, and there is a significant decrease in the g_z value. Note also that the $g_\perp$ of the type 2 site in the peroxide adduct is lower than both g_x and g_y of the resting type 2 site. There is also a significant change in the perpendicular hyperfine splitting $^{Cu}A_\perp$ with both $^{Cu}A_x$ and $^{Cu}A_y$ increasing and apparently becoming more rhombic in the peroxide adduct even though the *g* values associated with the adduct are axial.

(59) DuBois, J. L.; Mukherjee, P.; Collier, A. M.; Mayer, J. M.; Solomon, E. I.; Hedman, B.; Stack, T. D. P.; Hodgson, K. O. *J. Am. Chem. Soc.* **1997**, *119*, 8578.

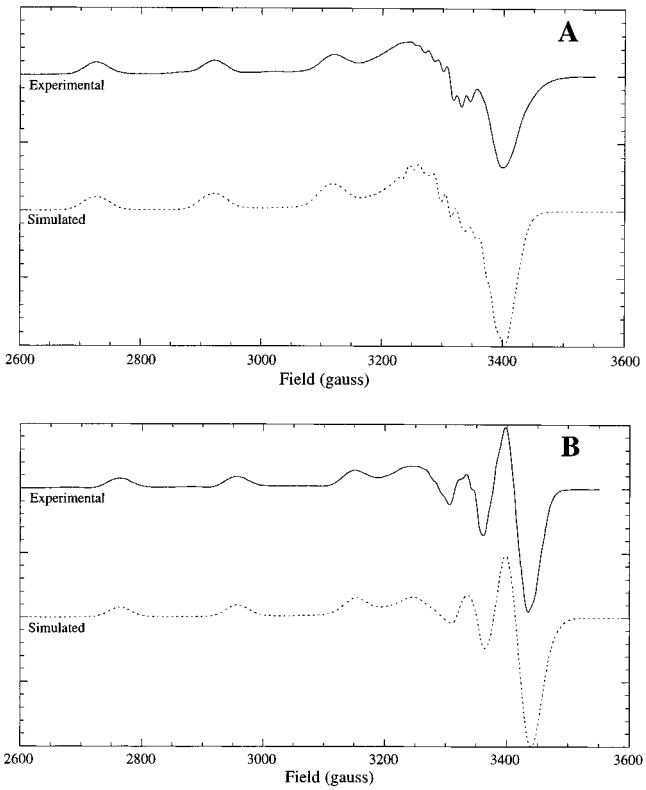

Figure 5. (A) (—) Experimental and (···) simulated spectra of resting T1Hg Lc. (B) (—) Experimental and (···) simulated spectra of the peroxide adduct of T1Hg Lc. The experimental EPR spectra were recorded under the following conditions: microwave power, 20 mW; modulation amplitude, 20 G; modulation frequency, 100 kHz; microwave frequency, 9.512 GHz; time constant, 0.5 s. Spin Hamiltonian parameters obtained from the simulations are in Table 2.

These changes in the type 2 EPR spectrum occurring on H_2O_2 addition along with the result that peroxide does not bind either on removal of the type 2 Cu (the T2D derivative), or when F^- is bound to this center (*vide supra*), suggest that H_2O_2 binds to the type 2 center. Binding to the type 2 center is further required by the charge-transfer (CT) analysis in section VI. The *g* and *A* values of the resting and peroxide-bound T1Hg Lc obtained through the simulations (Table 2) can be analyzed to investigate the nature of changes occurring at the type 2 site on formation of the peroxide adduct.

The ligand field expressions for *g* value are given below:[60]

$$g_x = 2.0023 - \frac{2\lambda k_x^2 (a - \sqrt{3}b)^2}{\Delta E_{yz}}$$

$$g_y = 2.0023 - \frac{2\lambda k_y^2 (a + \sqrt{3}b)^2}{\Delta E_{xz}} \qquad (1)$$

$$g_z = 2.0023 - \frac{2\lambda k_z^2 a^2}{\Delta E_{xy}}$$

where k_i represents the Stevens orbital reduction factor, λ is the spin−orbital coupling constant (which is -830 cm^{-1} for d^9 Cu (II)), *a* and *b* are the coefficients of $d_{x^2-y^2}$ and d_{z^2} in the ground state, respectively, and the denominators are transition energies from the d_{yz}, d_{xz}, and d_{xy} levels (to the $d_{x^2-y^2}$ level) for g_x, g_y and g_z, respectively. The second term on the right in these expressions is a measure of the orbital angular momentum

(60) McGarvey, B. R. *Transition Met. Chem. (N. Y.)* **1966**, *3*, 89.

Table 2. EPR Simulation Parameters of Resting and Peroxide Adduct of T1Hg Lc

	g value			^{Cu}A value ($\times 10^{-4}$ cm^{-1})			^{N}A value ($\times 10^{-4}$ cm^{-1})			line width ($\times 10^{-4}$ cm^{-1})		
sample	g_z	g_x	g_y	$\|A_z\|$	$\|A_x\|$	$\|A_y\|$	$\|A_z\|$	$\|A_x\|$	$\|A_y\|$	L_x	L_y	L_z
resting	2.252	2.070	2.040	205	17	17	10	17	10	8	12	12
adduct	2.225	2.032	2.032	202	31	45	10	10	12	15	15	15

contribution, the decrease in which would lead to *g* values closer to the spin only value of 2.0023.

We first consider the decrease in all the *g* values on going from the resting to the peroxide adduct form. This reflects a reduction in orbital angular momentum of the ground-state wave function (unpaired electron in $d_{x^2-y^2}$). This can result from an increase in ligand field splitting of d-orbitals and an increase in ligand character (i.e., increase in covalency, which decreases k_i) in the ground-state wave function. The experimental ligand field transition energies of the type 2 copper do in fact increase in the peroxide adduct (from MCD data, *vide infra*), indicative of an increase in the ligand field strength at the type 2 copper. To fully account for the experimentally observed decrease in *g* values, a further reduction in the orbital angular momentum contribution to the *g* values has to occur and this requires a reduction in the Stevens orbital reduction factor. The decrease in *g* values is thus consistent with an increase in ligand field strength at the type 2 site and an increase in its covalency, both of which are consistent with the addition of peroxide ligand resulting in the type 2 center going from a 3- to 4-coordinate site.

The change from rhombic to axial g_x and g_y indicates equalization of ligand interactions along *x* and *y* directions in the adduct, relative to the resting site. From eq 1 this could be due to (a) a decrease in the energy splitting of the d_{xz} and d_{yz} states and (b) a decrease in the amount of d_{z^2} mixing in the $d_{x^2-y^2}$ ground state. From the MCD spectra (*vide infra*) of resting and peroxide adduct of T1Hg Lc, the d_{xz} and d_{yz} levels are less split in the adduct relative to resting protein, causing the energy denominator ΔE_{xz} and ΔE_{yz}, and consequently g_x and g_y, to be more equal. Further, from *A* value calculations (*vide infra*), the amount of d_{z^2} mixing in the ground-state wave function decreases from ~0.5% in resting T1Hg Lc to ~0% on going to the peroxide adduct. This reduction in d_{z^2} mixing indicates a higher symmetry site (~D_{4h}) also consistent with a more square planar type 2 site in the adduct.

The hyperfine coupling constant has contributions from Fermi contact, direct spin dipolar, and indirect orbital dipolar coupling terms. The apparent axial splitting of *A* values for the rhombic type 2 site in resting and rhombic splitting of the ^{Cu}A values for an axial type 2 site in the adduct and the changes in *A* values on going from the resting to the peroxide adduct site can be analyzed in terms of the following *A* value expressions:[60,61]

$$A_x = P_d\left[-\kappa + \frac{2\alpha^2(a^2-b^2)}{7} + \frac{\alpha^2 4ab\sqrt{3}}{7} + (g_x - 2.0023) - \frac{(3a-\sqrt{3}b)(g_y-2.0023)}{14(a+\sqrt{3}b)} - \frac{b(g_z-2.0023)}{7a}\right]$$

$$A_y = P_d\left[-\kappa + \frac{2\alpha^2(a^2-b^2)}{7} - \frac{\alpha^2 4ab\sqrt{3}}{7} + (g_y - 2.0023) - \frac{(3a+\sqrt{3}b)(g_x-2.0023)}{14(a-\sqrt{3}b)} - \frac{b(g_z-2.0023)}{7a}\right] \quad (2)$$

$$A_z = P_d\left[-\kappa - \frac{4\alpha^2(a^2-b^2)}{7} + \frac{(3a-\sqrt{3}b)(g_y-2.0023)}{14(a+\sqrt{3}b)} + \frac{(3a+\sqrt{3}b)(g_x-2.0023)}{14(a-\sqrt{3}b)} + (g_z - 2.0023)\right]$$

using experimental *g* values. The α^2 (percent metal character in the ground-state wave function reduced from 1.0 due to covalent electron delocalization onto the ligand orbitals), κ (Fermi contact contribution due to spin polarization) and *a* and *b* (the $d_{x^2-y^2}$ and d_{z^2} contribution to the ground-state wave function) were systematically varied until the best fit to the experimental *A* values was achieved (P_d was fixed at 400 $\times$ 10^{-4} cm^{-1} for Cu^{2+}), and the results are presented in Table 3. The fit between the experimental and calculated values is good, and it is seen that the A_z value remains almost the same, while there is a significant increase in the magnitudes of A_x and A_y on going to the peroxide adduct. The sign of the *A* values are obtained from the calculations, but not from experiment. For the resting site, A_z and A_x are negative while A_y is positive, while for the peroxide adduct site, all the *A* values are negative. Thus, even though the A_x and A_y splitting appears to be axial for the rhombic resting type 2 site, it is in fact rhombic with $\Delta A = 34 \times 10^{-4}$ cm^{-1} (since they are of opposite sign) and is closer to axial for the adduct site with ΔA being only 13×10^{-4} cm^{-1}. The difference in A_x and A_y derives from d_{z^2} mixing (~0.5% in resting and ~0.06% in the adduct) with the third term in eq 2 above being of opposite sign in the A_x vs A_y expressions. Additionally, in the resting site, the rhombicity of *g* values contributes to the rhombicity in *A* values.

The increase in magnitude of A_x and A_y on going from the resting site to the peroxide adduct derives from (a) a decrease in α^2 from 0.88 to 0.73 (which decreases the opposing positive contribution from the spin dipolar term) which indicates an increase in covalency of the site on going to the adduct, (b) the decrease in *g* values (discussed above) which decreases the positive contribution from the orbital dipolar term, (c) a decrease in d_{z^2} mixing, and (d) an increase in κ which increases the negative contribution from the Fermi contact term. The value of κ depends on spin polarization, which is indirect and negative for an electron in $d_{x^2-y^2}$ orbital but direct and positive for an electron in a 4s orbital. The increase in κ in the adduct is thus indicative of a shift from a site of lower symmetry (where 4s mixing into the $d_{x^2-y^2}$ orbital is allowed) to one of higher symmetry (where 4s mixing into the $d_{x^2-y^2}$ orbital is forbidden); the magnitude of the change in κ would be accounted for by a decrease in 4s mixing by ~1%. This is consistent with the resting 3-coordinate ~C_{2v} type 2 site going to a 4-coordinate ~D_{4h} structure through the addition of a ligand at the open coordination position of the type 2 Cu.

Summarizing the results from 77 K EPR, the changes in *g* and *A* values indicate addition of a ligand at the open coordination position of the type 2 site resulting in a more symmetric, 4-coordinate, ~D_{4h} structure.

Low-temperature (6.5 K), high-power (200 mW) EPR studies were performed on the resting and peroxide-bound forms of

(61) Wilcox, D. E.; Porras, A. G.; Hwang, Y. T.; Lerch, K.; Winkler, M. E.; Solomon, E. I. *J. Am. Chem. Soc.* **1985**, *107*, 4015.

Table 3. Experimental and Calculated Cu Hyperfine Values

	$\lvert^{Cu}A\rvert$ value ($\times 10^{-4}$ cm^{-1}) (exptl)			^{Cu}A value ($\times 10^{-4}$ cm^{-1}) (calcd)					
sample	$\lvert A_z\rvert$	$\lvert A_x\rvert$	$\lvert A_y\rvert$	A_z	A_x	A_y	κ	α^2	$\%d_{z^2}$
resting	205	17	17	−205	17	−17	0.29	0.87	0.5
adduct	202	31	43	−202	−31	−43	0.328	0.73	0.06

T1Hg Lc. No new signals were observed even when the pH was lowered to 4.6 (0.1 M sodium acetate). The signals under nonsaturating conditions, for both resting and peroxide adduct of T1Hg Lc, quantitated to be the same amount of paramagnetism as at 77 K (∼0.95 spins). There is thus no indication of any dipolar coupled coppers even under low-pH, high-power conditions or any increase in paramagnetism even at low temperature (6.5 K). This lack of change in the amount of paramagnetism both at 77 K and at He temperatures (under nonsaturating conditions) indicates that the antiferromagnetically coupled type 3 site still remains EPR silent, and no change in the magnetic state of the trinuclear cluster is observed. The saturation behavior of the type 2 site has however been altered by peroxide binding (see the Supporting Information), which is consistent with peroxide perturbing the energy levels of the type 2 site as observed below.

Note that SQUID magnetic susceptibility studies were attempted on resting and peroxide-bound forms of T1Hg Lc to determine the magnetic coupling within the trinuclear cluster in the resting state and peroxide adduct form. For resting T1Hg Lc, only one Cu^{2+} contributes to the magnetic susceptibility up to 100 K. This magnetism is associated with the EPR detectable type 2 Cu^{2+}, and these data indicate that the type 3 coppers remain diamagnetic up to 100 K. Earlier susceptibility studies on laccase[7,9,10] gave a lower limit for the singlet−triplet energy splitting of $-2J > 400$ cm^{-1}. For the peroxide adduct site, SQUID susceptibility data could not be reproducibly obtained due to the large amount of dissolved oxygen (produced by disproportionation of the peroxide in the protein solution) which could not be corrected for in the background sample. Also, the presence of dissolved O_2 resulted in bubbles in the sample which caused density changes that precluded any reliable measurement of volume susceptibility, the quantity measured in the experiment.

IV. Ligand Field Region: Absorption, CD, and MCD. Ascorbate is known to reduce the type 2 site faster than the type 3 site.[62] This allows samples of T1Hg Lc to be prepared in which the type 2 is selectively reduced. Figure 6A,B shows the effect of this reduction on the CD and EPR spectra. While a 75% reduction in the type 2 EPR intensity occurs, no significant change in the CD spectrum is observed between the resting and ascorbate-reduced T1Hg Lc. This suggests that the type 2 site contributes little to the CD spectrum of T1Hg Lc which is dominated by contributions from the type 3 center. Thus, within the trinuclear site, room temperature (RT) CD selectively probes the type 3 site and LT MCD selectively probes the paramagnetic type 2 site (*vide infra*).

Figure 7 shows the CD spectra in the ligand field region of resting (dotted line) and peroxide-bound (solid line) T1Hg Lc (see the Supporting Information for their simultaneous Gaussian resolutions with absorption and MCD spectra in this region). The band energies along with their intensities and signs are given in Table 4. The resting spectrum has five ligand field bands which implies that the two type 3 coppers are inequivalent[10,19] (see section V). The adduct spectrum also shows five bands but at higher energies, with different intensities and in some cases with different signs relative to the resting CD spectrum. Thus peroxide addition perturbs the type 3 ligand field, suggesting that this ligand binds to the type 3 site. Also the ligand field spectra of the peroxide adduct indicates that the copper(II)'s are not being further oxidized with peroxide addition. This together with the reversibility of H_2O_2 binding and the lack of any short Cu−oxygen distance in the fit to the EXAFS data of the adduct (section II) strongly suggests that peroxide is binding intact and that the adduct does not contain a Cu(III)−oxo type of species.

LT MCD selectively probes paramagnetic centers; hence only the type 2 site contributes to the LT MCD spectrum. Figure 8 shows the 4.2 K MCD spectrum of the resting (dotted line) and

(62) Tamilarasan, R.; McMillin, D. R. *Biochem. J.* **1989**, *263*, 425.

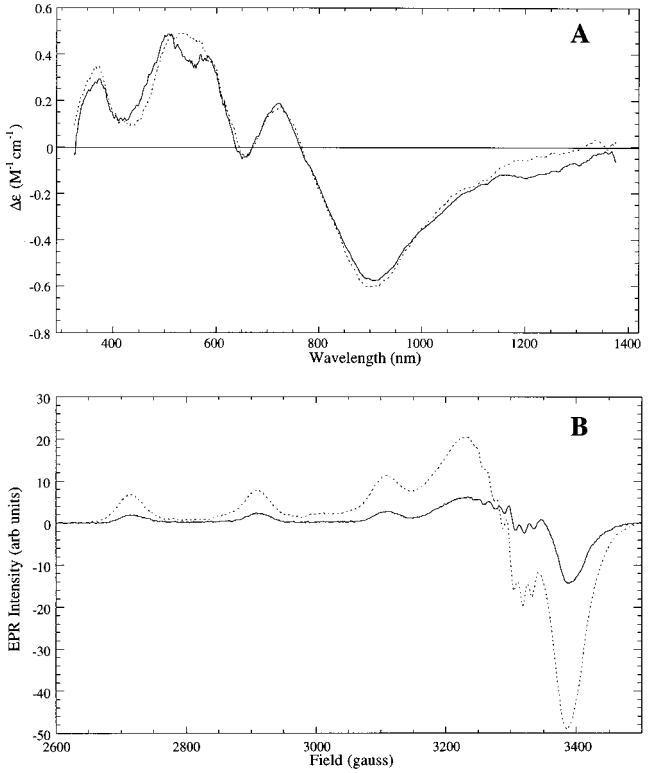

Figure 6. (A) Room-temperature CD of (- - -) resting T1Hg Lc and (—) ascorbate-reduced T1Hg Lc. (B) CD samples monitored by EPR at 77 K.

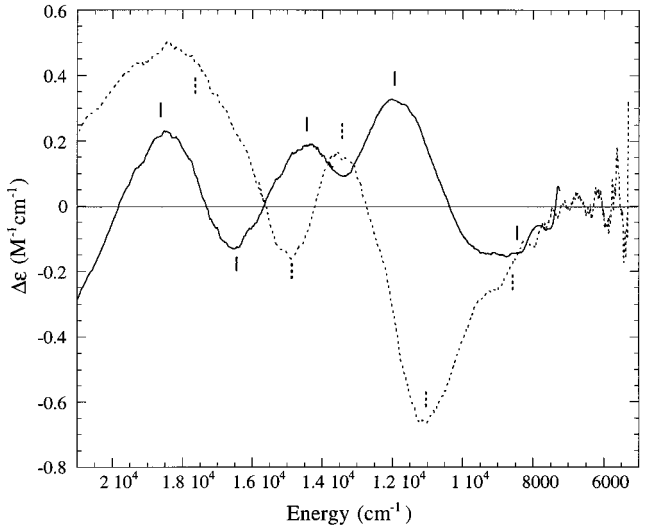

Figure 7. Room-temperature CD spectra in the ligand field region of (···) resting T1Hg Lc and (—) T1Hg Lc + 200-fold excess of H_2O_2. The positions of bands in both resting (dotted) and peroxide adduct (solid) spectra are marked.

Table 4. Absorption and CD and MCD Bands in the Ligand Field Region

resting T1Hg Lc		peroxide adduct of T1Hg Lc	
energy (cm^{-1})/nm	intensity	energy (cm^{-1})/nm	intensity
Absorption			
12300/813	150	13265/754	97
13800/725	130	14900/671	185
15150/660	050	16400/610	292
18280/547	015	19000/526	112
RT CD			
9150/1093	(−)0.10	9090/1100	(−)0.175
11065/903	(−)0.60	11960/836	(+)0.32
13890/720	(+)0.18	14500/690	(+)0.21
15275/655	(−)0.96	16810/595	(−)0.16
17386/575	(+)0.38	18447/542	(+)0.23
LT MCD			
9400/1067	(+)0.19	11815/846	(+)1.0
12100/826	(+)0.36	12932/773	(−)1.05
14134/708	(−)1.25	17340/577	(+)1.7
18419/543	(−)1.10	19701/507	(−)2.5

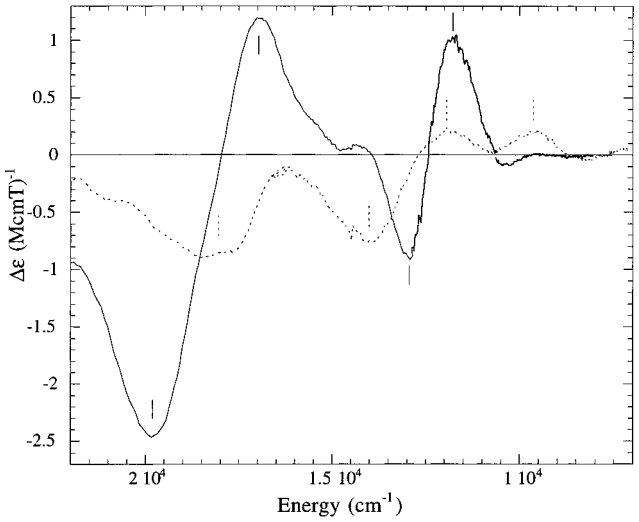

Figure 8. 4.2 K MCD spectra in the ligand field region of (···) resting T1Hg Lc and (—) T1Hg Lc + 200-fold excess of H_2O_2. The position of bands in both (···) resting and (—) peroxide adduct spectra are marked. [The spectra have been corrected for ∼2% native contaminant in the T1Hg Lc preps (determined by activity measurements) and for 20% resting form that is present in the sample under these conditions based on the equilibrium binding constant and renormalized.

peroxide adduct (solid line) of T1Hg Lc in the ligand field region. The peak positions of the bands are marked in resting and in the peroxide adduct spectra with the energy position, intensity, and sign of the bands given in Table 4. Note that the T1Hg Lc preps have ∼2% native Lc contaminant, which has an intense MCD band at 16 000 cm^{-1}, which has been subtracted from the data of both resting and adduct. Additionally the MCD spectrum of the adduct is corrected for ∼30% unconverted resting T1Hg Lc and renormalized. These corrections result in small spectral features, in particular a shoulder at ∼15 500 cm^{-1}. The MCD bands in both show C-term behavior (i.e., decrease in intensity with increase in temperature), indicating that they arise from an $S = {}^1/_2$ species (the type 2 Cu(II) center). All four d−d bands in the resting site change in energy, intensity, and sometimes sign. There is mostly an increase in energy and intensity which is consistent with an increase in ligand field strength, reflective of ligand binding to the paramagnetic type 2 center. No new d−d bands, which might occur if the type 3 center became paramagnetic, are observed. The increase in intensity of the highest energy d−d band is consistent with

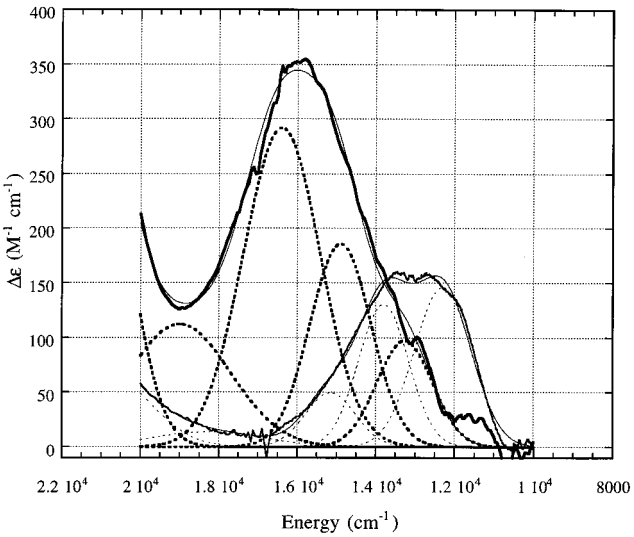

Figure 9. Room-temperature absorption spectra in the ligand field region of (—) resting T1Hg Lc and (···) T1Hg Lc + 200-fold excess of H_2O_2. The thin dotted and thick dotted spectra are the Gaussian resolved bands (based on simultaneous fit with RT CD and LT MCD spectra in this region) of the resting and peroxide adduct spectra, respectively.

mixing with a new low-energy $O_2^{2-} \rightarrow$ Cu(II) charge-transfer band present in the adduct (*vide infra*). The MCD results thus corroborate the EPR results in that binding to the type 2 site is indicated with the type 3 site still remaining strongly antiferromagnetically coupled.

Figure 9 gives the absorption spectra in the ligand field region of resting (thin, solid line) and peroxide adduct (thick, solid line) along with their Gaussian resolution (dotted lines), based on simultaneous fitting of the absorption, CD, and MCD spectra in this region (see the Supporting Information), with the energy position of the bands along with their intensities given in Table 4. As seen from a comparison of bands in absorption, CD, and MCD, except for the band at 12 300 cm^{-1} in absorption which correlates with the 12 100 cm^{-1} band in the MCD, the other two Gaussian resolved bands in the absorption spectra correlate with bands in the CD. Thus it appears that the predominant contribution to the ligand field absorption is the type 3 center. This is supported by the fact that this ligand field absorption band is lacking in the type 3 reduced form of T2D and is recovered on oxidation of the type 3 center.[55] Thus this ligand field band is present in both type 1 and type 2 eliminated forms of the protein and must be associated with the type 3 center. That the type 3 d−d transitions dominate the CD spectrum then appears to correlate with the high intensity of the absorption spectrum since CD intensity is proportional to the product of electric and magnetic dipole transition probabilities. This dominance of the type 3 center in absorption is likely due to a lowered site geometry of this site relative to the type 2 site which is close to planar. On peroxide addition, these ligand field absorption bands move to higher energy (clearly seen in the difference absorption titration data (Figure 1B); an isosbestic point is found at ∼685 nm (15 900 cm^{-1})). While all the Gaussian resolved bands move to higher energy, the ones which correlate with the CD (hence type 3 related) show an increase in intensity. The increased intensity of the type 3 d−d in the peroxide adduct is likely due to mixing with low-energy peroxide → Cu(II) CT transitions associated with this site. There is also a substantial increase in intensity in all the four ligand field MCD bands on going from the resting to adduct. This intensity mixing is likely due to spin−orbit mixing with a new charge-transfer state. At least in the case of one of the MCD

bands (at ~12 100 cm^{-1}), which can be clearly correlated with an absorption band at the same energy, there is no increase in absorption intensity. Mixing of states due to a lower symmetry in the adduct is therefore eliminated as the cause for the increased MCD intensity. This requires an increased C/D ratio which could be due to spin−orbit mixing with either the excited state (ES) or the ground state (GS). An increase in intensity is observed for bands with both positive and negative intensity; therefore, spin−orbit mixing into the ground state is eliminated as the cause for the increased MCD intensity. Spin−orbit mixing between ESs can occur, due to a decreased energy splitting between states, a decrease in the covalency, or mixing with new CT ESs. There are small shifts in energy splittings between ligand field (LF) excited states in the adduct relative to resting, with an overall small decrease in splitting of ~400 cm^{-1}. This is insufficient to account for the observed average increase (of ~3 times) in intensity. There is an increase, not decrease, in covalency of the site in the adduct from the EPR hyperfine values (see Table 3). Thus, spin−orbit mixing with a new CT state is likely the cause of the increased intensity of the ligand field bands in the MCD spectrum. Both the MCD transitions, which are due to the paramagnetic type 2 copper, and the ligand field absorption, which is predominantly due to the type 3 coppers, show an increase in intensity which appears to be due to CT mixing with the peroxide bound to the trinuclear site. Since CT intensity requires orbital overlap, this suggests that peroxide binds to both type 2 and type 3 centers. Direct evidence for CT transitions to the type 2 and type 3 coppers is discussed in section VI.

V. Ligand Field Calculations. Having a combination of spectral data and a crystallographically defined trinuclear copper site geometry, an initial electronic structure description of the trinuclear site can be generated by means of a ligand field analysis. This description helps in understanding the origin of the strong antiferromagnetic coupling between the type 3 coppers and the orientation of the imidazoles (of the type 3) involved in the electron-transfer pathway to the type 1[4,14] and gives insight into modes of exogenous ligand binding at the trinuclear site.

The energy levels and wave functions were calculated using the method of Companion and Komarynsky.[63] The initial values for the ligand field parameters α_2 and α_4 (not to be confused with α,[2] the term denoting covalency in the EPR analysis (*vide supra*)) were determined from $Cu(Imidazole)_4$ and $Cu(H_2O)_6$ model complexes.[61,64−66] The values of α_2 and α_4 were systematically varied for each model complex until the set of values which produced the best match between the calculated energy level splitting and the experimental ligand field optical spectra (Figures 7 and 8) were obtained. These values were then extrapolated to the metal−ligand bond distances found in the crystallographically defined protein active site using the approximation that α_2 and α_4 are proportional to $1/R^3$ and $1/R^5$, respectively, where R is the bond length, and then these were adjusted to fit the experimental data on the resting and peroxide adduct forms of T1Hg Lc.

The resting type 2 site has a square planar geometry with an open coordination position in the equatorial plane directed toward the two type 3 coppers. The ligands are two imidazoles and one H_2O (rather than a hydroxide based on its pK_a between 6 and 7[62]). This site has the $d_{x^2-y^2}$ orbital highest in energy, and on the basis of the hole formalism, the ordering of the d states is as shown in the energy level diagram in Figure 10A (left) (the levels on the *y* axes are experimental, and those in the center are calculated as labeled in the figure). The correlation between the experimental and calculated values for the resting type 2 site is very reasonable. For the resting type 3 site, both coppers are ~trigonal bipyramidal (tbp) with an open coordination position in the equatorial plane of the tbp, oriented toward the open coordination position of the type 2 site. The ~tbp geometry for the type 3 coppers derives from the almost linear Im(N)-Cu−OH (bridge) bond angle for both type 3 coppers. For this site, the d_{z^2} orbital is highest in energy and the ordering of the 1-hole states are as shown in Figure 10B (center and right) for the two resting type 3 coppers with the experimental levels shown on the left *y* axis. This initial electronic structure description is superimposed on the crystal structure of the trinuclear site of AO in Figure 11. The type 2 site has been rotated by 90° (as indicated in the figure) for clarity of viewing. Note that the lobes of the d_{z^2} orbital of the type 3 coppers overlap with the p orbital of the bridging hydroxo ligand, providing a good superexchange pathway, which is responsible for their strong antiferromagnetic coupling. One of the equatorial imidazole ligands (on each type 3 copper) is

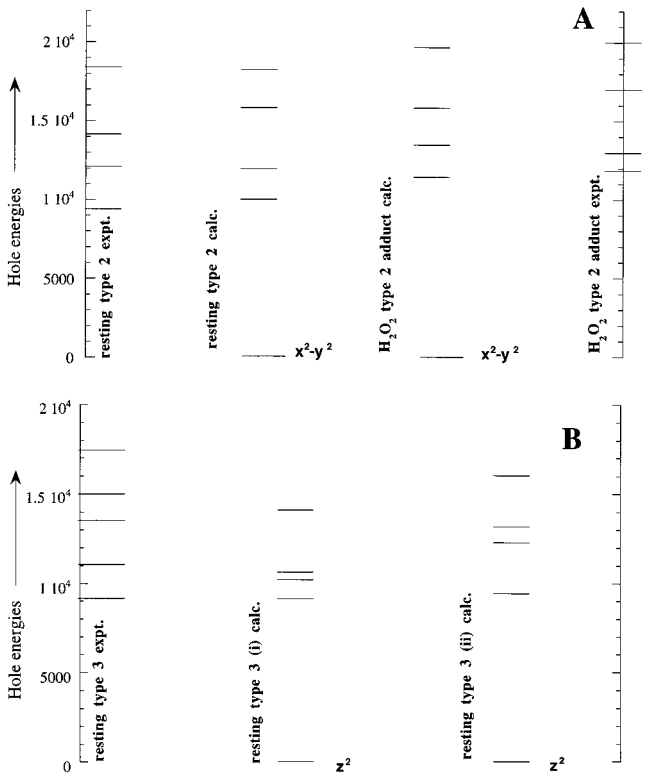

Figure 10. (A) Ordering of the one-hole states for the type 2 Cu(II) site. The levels on the *y* axis on the left are the experimentally obtained d−d energies for the resting type 2 site (from LT MCD). The levels on the *y* axis on the right side are experimentally obtained d−d energies for the type 2 site in the peroxide adduct (from LT MCD). The calculated levels are shown: (left) the resting type 2 site (using the crystal coordinates of AO) and (right) type 2 site to which a peroxo ligand was added to the open equatorial coordination position. (B) Ordering of the one-hole states for the two type 3 Cu(II)'s. The levels on the *y* axis (left) are the experimentally obtained levels for the type 3 site (from RT CD, see text). The calculated levels, using the crystal coordinates of oxidized AO, are shown to the right for type 3 Cu(i) and type 3 Cu(ii). The ground state for the type 2 and type 3 sites is indicated in each figure.

(63) Companion, A. L.; Komarynsky, M. A. *J. Chem. Educ.* **1964**, *41*, 257.

(64) Penfield, K. W.; Gay, R. R.; Himmelwright, R. S.; Eickman, N. C.; Norris, V. A.; Freeman, H. C.; Solomon, E. I. *J. Am. Chem. Soc.* **1981**, *103*, 4382.

(65) Hitchman, M. A.; Waite, T. D. *Inorg. Chem.* **1976**, *15*, 2150.

(66) Brown, G. M.; Chidambaram, R. *Acta Crystallogr.* **1969**, *B25*, 676.

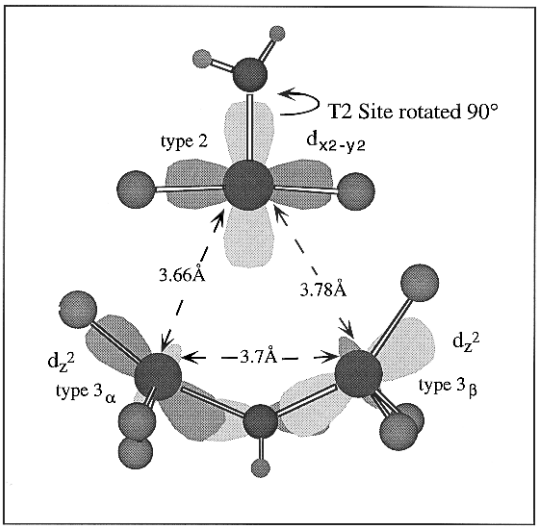

Figure 11. Trinuclear cluster site depicted using the crystal coordinates from AO. The appropriate ground states for the type 2 and type 3 sites, obtained from ligand field calculations, are superimposed as is the p-orbital of the bridging hydroxide oxygen. The type 2 site is rotated by 90° for clarity.

involved in the type 1−Cys-His−type 3 electron-transfer pathway.[4,14]

The two type 3 sites are inequivalent. This is evident from the fact that there are at least 5 d−d bands arising from the type 3 site (see Figure 7). This was predicted on the basis of spectroscopy[10] and pointed out in the crystallography[19] as being due to the bonding of one of the imidazole ligands through its δ- instead of its ϵ-nitrogen. The ligand field calculations for the two type 3 coppers of the resting trinuclear site indicate that the inequivalent ligand fields for the two type 3 centers arise because one of the imidazole−Cu bonds is shorter than the average of the rest, causing that type 3 copper to have a stronger ligand field. The bond angles and bond lengths (through changes in the radial integrals α_2 and α_4) were systematically varied to make one of the type 3 coppers equal to the other. The factor which had the largest effect was the presence of the short Cu−Im bond (and therefore larger α_2 and α_4) on one Cu. This short bond is the imidazole bonded through its δ-nitrogen atom. From Figure 10B, for both coppers of the resting type 3 site, the correlation between the calculated (middle and right) and experimental (left *y* axis) values is quite reasonable.

A peroxo ligand was placed in the open coordination position of the type 2 site and ligand field calculations were performed (using a bond length of 1.95 Å for the peroxo-type 2 copper bond, based on EXAFS) and correlated with the MCD ligand field bands obtained for the peroxo adduct. As shown in energy level diagram in Figure 10A (right), the correlation between the calculated and experimental levels is very reasonable with the bands moving to higher energy in the experimental spectrum as well as in the calculations, supporting a model with peroxo bound in the open equatorial position of the type 2 site which thus becomes 4-coordinate.

VI. CT Region: Absorption, CD, and MCD. Figure 12A−C shows the LT MCD, RT absorption, and RT CD spectra in the CT region of resting and peroxide-bound T1Hg Lc along with their Gaussian resolved bands, obtained by simultaneous fitting of absorption, CD, and MCD spectra. (The adduct spectra in absorption and CD are difference spectra, with the resting T1Hg Lc spectrum subtracted.) In the difference absorption spectrum shown in Figure 12B, there are *at least* two new intense CT bands arising due to the peroxo species at 29 616 cm^{-1} (338 nm, $\epsilon \sim 3200$ M^{-1} cm^{-1}) and 25 500 cm^{-1} (392 nm, $\epsilon \sim 3700$ M^{-1} cm^{-1}) and two less intense bands at 23 350 cm^{-1} (428 nm, $\epsilon \sim 1300$ M^{-1} cm^{-1}) and 21 700 cm^{-1} (461 nm, 600 M^{-1} cm^{-1}). This indicates that the peroxo species must bind to more than one copper since there can be at most one π^*_σ and one π^*_v (for a total of two) peroxide to Cu(II) CT bands for binding to a single Cu(II) ion. The presence of two intense bands suggests that there are σ bonding interactions of the peroxo ligand with *two* Cu(II)'s. This spectrum in Figure 12B looks very similar to that obtained for the T1Hg Lc oxygen intermediate[32] with an additional band in the peroxide adduct at ∼25 500 cm^{-1} (392 nm). There is a band in the LT MCD spectrum at the same energy, but none in the RT CD spectrum (comparing Figure 12A−C). Since LT MCD intensity requires a paramagnetic site, this clearly indicates that the 392 nm CT band is due to a O_2^{2-} CT transition to the paramagnetic type 2 center (which is oxidized in the adduct, but reduced in the T1Hg Lc oxygen intermediate[32]). Thus the peroxide must be bound to the type 2 center.

Further, the ∼29 500 cm^{-1} band in the absorption spectrum has little or no MCD intensity associated with it. The C/D ratio for this band is estimated to be more than 1 order of magnitude lower than that for the 25 500 cm^{-1} MCD band, indicating that the 29 500 cm^{-1} band is not associated with a paramagnetic copper. Also, on comparing the CT absorption spectra of the T1Hg Lc oxygen intermediate and the peroxide adduct (*vide infra*), there is a band at ∼29 400 cm^{-1} in both. The peroxide adduct of T1Hg Lc can be correlated with the T1Hg Lc oxygen intermediate with the type 2 copper oxidized. Therefore an internally consistent assignment for the 29 500 cm^{-1} CT absorption band in the adduct is that it is CT from O_2^{2-} to the type 3 site which is antiferromagnetically coupled and has no LT MCD intensity associated with it.

There are two to three additional CT bands in the MCD spectrum which could at least in part be due to endogenous imidazole → type 2 Cu(II) CT transitions which are also present in the resting type 2 spectrum (dotted line in Figure 12A). From the energy level diagram in Figure 10A, peroxide binding increases the energy of the $d_{x^2-y^2}$ orbital and likely causes the endogenous imidazole to type 2 Cu(II) CT transitions to shift to higher energy. [The CT transitions in the resting type 2 spectrum are likely due to the imidazole rather than the H_2O ligand since there is no change in these bands over the pH range of 5−8 while the pK_a of the coordinated H_2O is ∼6−7[62]]. There is a substantial increase in intensity of these CT bands. This higher intensity could be related to a higher metal content for these CT transitions. An increase in covalency is observed on going from the resting to the adduct (the α^2 value in section IV decreases from 0.87 in resting to 0.73 in the adduct). It could also derive from spin−orbit coupling with the new O_2^2 → type 2 Cu(II) CT transition present in the adduct.

Thus, the 25 500 cm^{-1} band is clearly a O_2^2 → type 2 Cu(II) CT transition and the 29 500 cm^{-1} must be assigned as a O_2^{2-} → type 3 Cu(II) CT transition. Therefore, the comparative analysis of the absorption, CD, and MCD spectra of the peroxide adduct in the CT region provide definitive evidence for peroxide binding to both type 2 and type 3 coppers; combined with the 3.4 Å bridging interaction in the EXAFS and with the EPR, ligand field CD and MCD, and absorption spectral data, these indicate that there is a bridging interaction between the type 2 and type 3 coppers.

Resonance Raman experiments were attempted on the peroxide adduct of T1Hg Lc, but the excess hydrogen peroxide present in the sample (necessitated by the low binding constant)

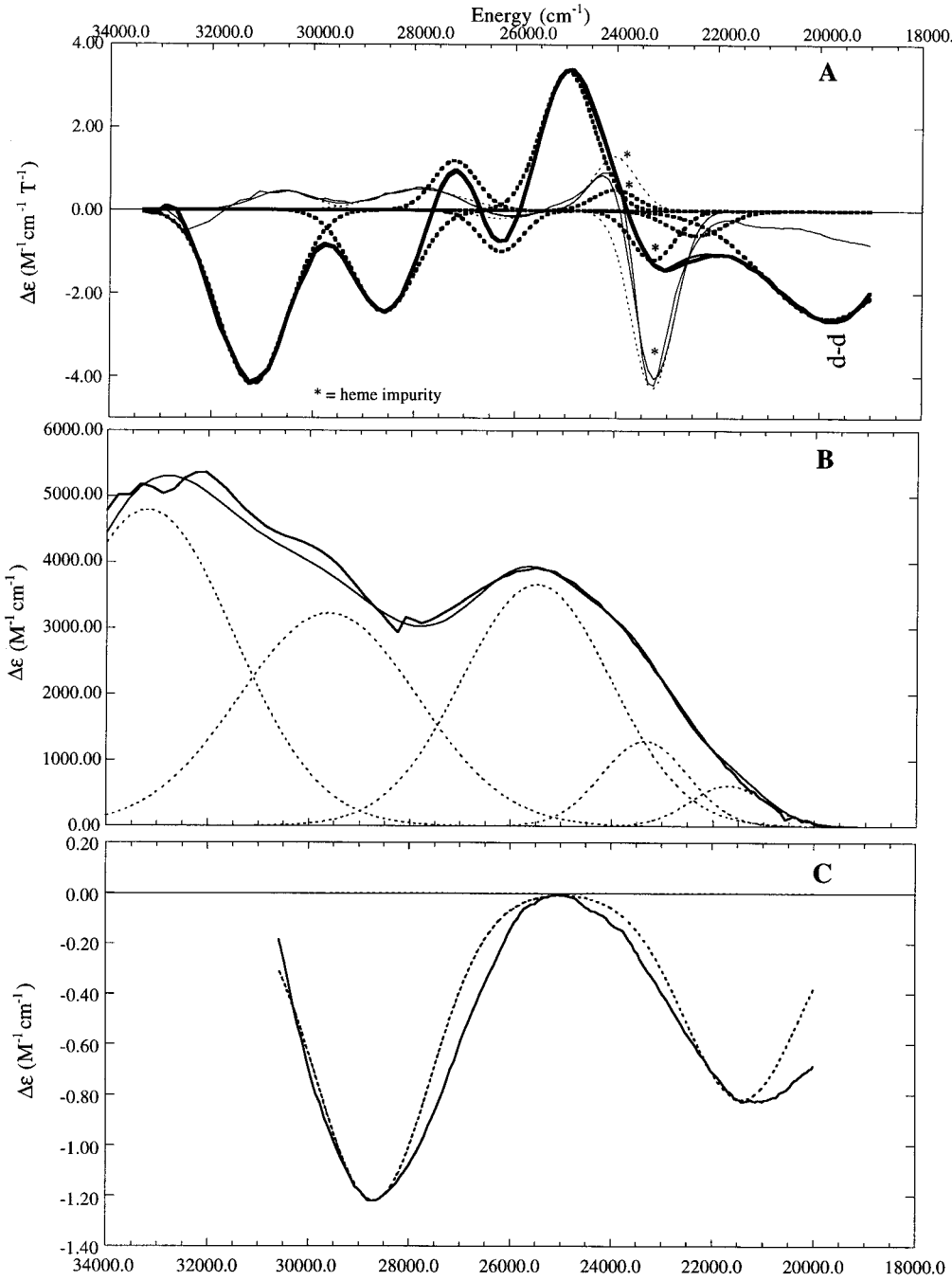

Figure 12. (A) LT MCD spectra in the charge-transfer region of (···) resting T1Hg Lc and (—) T1Hg Lc + 200-fold excess of H_2O_2 with band positions indicated in both. (B and C) Absorption and RT CD difference spectra, respectively, in the charge-transfer region after subtraction of resting T1Hg Lc. The spectra have also been corrected for 2% native Lc and ~25% unreacted resting T1Hg Lc. The position of bands in the difference adduct spectra are indicated.

gave an intense ν_{O-O} signal, obscuring observation of any peroxide stretch from the protein−peroxide adduct species.

Discussion

In this study, we have established that peroxide binds with a low-affinity ($K_B \sim 12\ M^{-1}$) to the fully oxidized trinuclear site, producing an adduct which is geometrically similar to the oxygen intermediate of T1Hg Lc,[32] the difference being the oxidation state of the type 2 copper which is reduced in the oxygen intermediate and oxidized in the peroxide adduct. Also, in both the peroxide adduct and in the oxygen intermediate of T1Hg Lc,[32] the bound oxygen species is not reduced beyond the peroxo level. This is indicated by the reversibility of H_2O_2 binding, by CT absorption spectral comparison to Cu(II)−peroxo vs Cu(III)−oxo complexes, and by the lack of evidence for a Cu(III)−oxo species from the edge and EXAFS data. Thus the oxygen intermediate of T1Hg Lc is indeed a peroxide intermediate which is similar to the peroxide adduct of T1Hg Lc with the type 2 copper oxidized in the latter.

The oxidized type 2 Cu center in the adduct could be probed by absorption, EPR, and MCD spectroscopies. Comparison of the absorption spectrum of the peroxide adduct with that of the oxygen intermediate of T1Hg Lc (Figure 13A), indicates that the spectrum of the adduct is similar to that of the intermediate with an additional band at ~392 nm assigned to $O_2^{2-} \rightarrow$ Cu(II) CT. This band has corresponding LT MCD intensity (see section VI) and thus is due to the paramagnetic type 2 copper; since CT intensity requires orbital overlap, this indicates O_2^{2-}

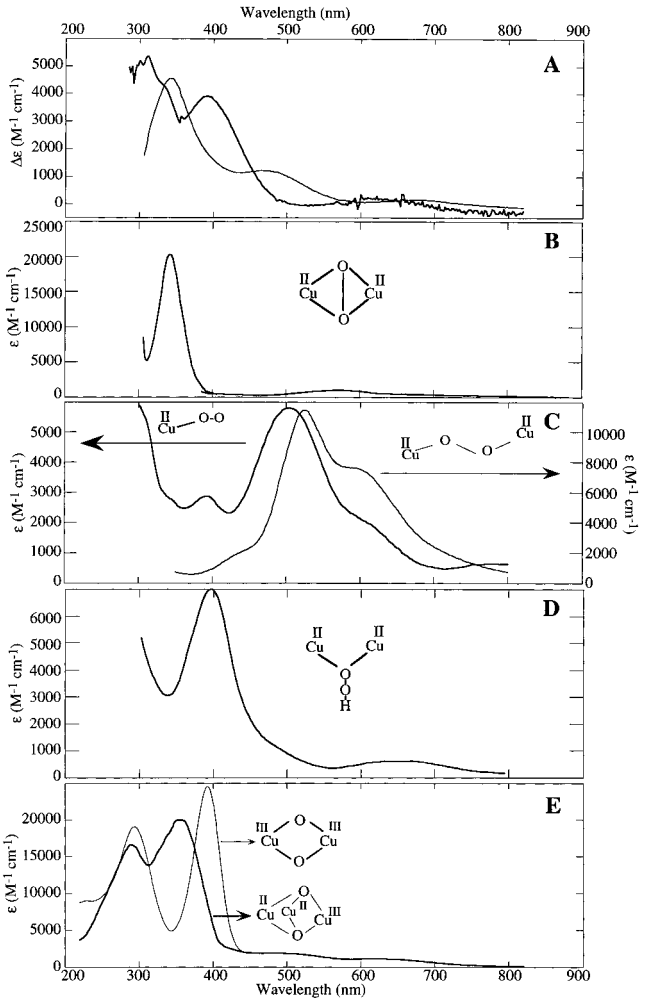

Figure 13. (A) Difference absorption spectra of the (thick solid line) peroxide adduct and (thin solid line) oxygen intermediate of T1Hg Lc. The difference is with respect to resting T1Hg Lc. The spectra have been renormalized to 100% adduct and intermediate. (B−E) Spectra of model complexes, with structural types indicated, reproduced from the following references: (A) ref 32; (B) refs 52 and 67; (C) refs 68 and 70; (D) ref 73; (E) refs 58 and 72.

coordination to the type 2 Cu(II). This is also supported by the fact that O_2^{2-} does not bind either in the absence of the type 2 (in the T2D derivative) or if F^- is bound to it. Significant changes occur in the EPR spectrum of the type 2 site on peroxide binding, which also indicate binding of peroxide to this site. All EPR *g* values decrease in the adduct relative to resting site, which indicates an increase in ligand field strength and covalency at the site. The change in g_x and g_y to axial in the peroxide adduct indicates change from unequal to equal interactions in the *x* and *y* directions consistent with the addition of a ligand at the open coordination position of the type 2. The increase in on going from the resting to the adduct is also consistent with an increase in coordination number of the type 2 site and a change from lower to higher symmetry (from $\sim C_{2v}$ to D_{4h}), indicating that the type 2 site goes from 3 → 4 coordinate. From LT MCD in the ligand field region, an increase in the energy of bands is observed on peroxide binding, indicating an increase in ligand field strength at the type 2 site in the adduct. This is corroborated by ligand field calculations of the peroxide bound type 2 site. The involvement of the type 2 Cu in binding the peroxo ligand firmly establishes the role of the type 2 center in catalysis.

The ligand field calculations on the resting trinuclear cluster have provided an initial electronic structure description of the trinuclear site. The type 2 Cu can be viewed as a square planar site lacking a ligand in the equatorial position having a $d_{x^2-y^2}$ ground state, and the two type 3 coppers can be described as having trigonal bipyramidal coordination each with a missing equatorial ligand and a d_{z^2} ground state with the open coordination positions of all three coppers oriented toward each other in the trinuclear copper cluster.

From the XAS data the peroxo ligand binds in a bridging mode between coppers. There is a new outer shell peak in the EXAFS spectrum at 3.4 Å in the peroxide adduct which is due to two coppers present at this distance, and the low Debye−Waller factor requires that they be rigidly bridged. This cannot be due to the type 3 coppers which are bridged by a hydroxide ligand, since the resting T1Hg Lc EXAFS data do not show this outer shell peak due to uncorrelated motion. From the absorption spectrum in the CT region, there are at least two O_2^{2-} → Cu(II) high-energy CT bands of fairly high intensity (at 338 and 392 nm, both with $\epsilon \sim 4000\ M^{-1}\ cm^{-1}$) and weaker low-energy bands at ∼ 430 nm ($\epsilon \sim 1300\ M^{-1}\ cm^{-1}$) and 460 nm ($\epsilon \sim 600\ M^{-1}\ cm^{-1}$). Both the intense bands are π^*_σ → Cu(II) CT transitions with the one at 392 nm being to the type 2 site (*vide supra*). Only one π^*_σ CT transition per Cu(II) can exist. The CT transition observed at ∼338 nm does not have corresponding LT MCD intensity; it is therefore not associated with a paramagnetic Cu center (*vide supra*). Further, it is similar in energy to the CT transition which occurs in the T1Hg Lc oxygen intermediate (∼340 nm) where the type 2 copper is reduced. Therefore an internally consistent assignment for the 338 nm (340 nm in the intermediate) CT band is that it is CT to the type 3 site. Further, from RT CD spectroscopy, which selectively probes the type 3 site the ligand field bands move to higher energy on peroxide addition. The absorption bands in the ligand field region of the resting protein (which are also primarily due to the type 3 copper) move to higher energy on peroxide addition, paralleling the changes in the RT CD in this region. Also these absorption bands show a significant increase in intensity which is likely due to mixing with O_2^{2-} CT states, and such an effect requires that these CT transitions be associated with the type 3 metal center. The new bridging interaction seen from the EXAFS data[32] requires that, in addition to binding to the type 2 Cu, the peroxide ligand must bind to the type 3 Cu and the above spectral data provide strong evidence for such a binding. Thus the peroxo ligand bridges between the type 2 and type 3 coppers.

A comparative analysis of the absorption CT spectra of the peroxide adduct and intermediate of T1Hg Lc with that of cupric peroxo and Cu(III)−oxo model complexes (Figure 13A−E with the structural types indicated within each panel) give some insight into the nature of this bridging mode. First, the CT absorption spectra of the peroxide adduct and intermediate (Figure 13A, thick and thin lines, respectively) are similar in both energy and intensity, with the adduct having an additional band at 392 nm due to the oxidized type 2 Cu (*vide supra*). Comparison of the CT spectrum of the peroxide adduct (Figure 13A, thick line) with that of the side-on μ-η^2: η^2 O_2^{2-}−Cu(II) complex[52,67] (Figure 13B) indicates that, while the higher energy π^*_σ CT transition occurs at about the same energy in both, the intensity is about 4−5 times higher in the side-on complex, reflecting the presence of additional Cu(II)−peroxide bonds in the latter. Relative to the end-on monomer[68,69] (Figure 13C,

(67) Kitajima, N.; Fujisawa, K.; Moro-oka, Y.; Toriumi, K. *J. Am. Chem. Soc.* **1989**, *111*, 8975.
(68) Karlin, K. D.; Cruse, R. W.; Gultneh, Y.; Farooq, A.; Hayes, J. C.; Zubieta, J. *J. Am. Chem. Soc.* **1987**, *109*, 2668.
(69) Pate, J. E.; Cruse, R. W.; Karlin, K. D.; Solomon, E. I. *J. Am. Chem. Soc.* **1987**, *109*, 2624.

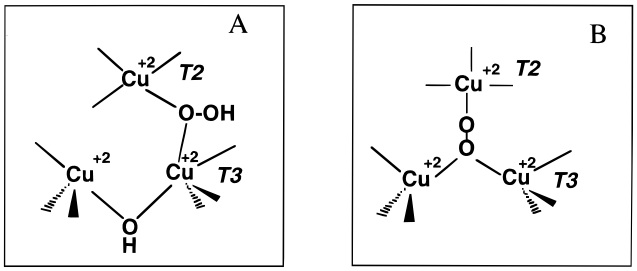

Figure 14. Two possible spectroscopically effective models for peroxide bridging at the trinuclear cluster site: (A) bridging between type 2 and one of the type 3 coppers in a μ-1,1-hydroperoxo mode; (B) bridging all three coppers in a μ_3, $(\eta^1)_3$ mode.

thick line), where the peroxo is bound terminally to one Cu(II) and to the trans μ-1,2 cupric dimer[70] (Figure 13C, thin line, which is predicted to be similar to the *cis* end-on dimer[71]), the bands in the adduct are to much higher energy. (The higher, ~2 times intensity of the trans μ-1,2 cupric dimer model relative to the end-on monomer relates to the presence of two bonding interactions in the former and one in the latter). The fact that both π^*_σ CT transitions in the adduct are higher in energy than the π^*_σ CT transition of the end-on monomer indicates additional bonding interaction in the adduct which would lower the energy of the ligand donor orbital and thus increase the energy of the CT transition. Comparing the CT spectra of the bis-μ-oxo Cu(III) dimer[58] and trimer[72] (Figure 13E, thick and thin lines, respectively) to the peroxide adduct the bands are 3−4 times higher in intensity. This argues against Cu(III)−oxo type species for the peroxide adduct of T1Hg Lc.

Comparing the hydroperoxo-bridged binuclear cupric model complex[73−75] (Figure 13D) with the adduct, the peroxide adduct spectrum is very similar to that of this model with an intense O_2^{2-} CT transition at 400 nm in both with a difference that there is one instead of two, π^*_σ transitions in the model. It is reasonable to explain this difference as being due to the equivalence of the two cupric centers in the hydroperoxo model complex which causes the CT transition to both Cu's to occur at the same energy in the model, while in the adduct, the two coppers to which CT transitions occur, the type 2 and type 3, have very different ligand fields and hence the O_2^{2-} −Cu(II) CT transitions to these cupric centers are expected to occur at different energies. Alternately, a splitting of the peroxo donor orbitals would also cause the CT transitions to occur at different energies. Thus, based on the similarities of the adduct spectrum to the one in 13D, one possible binding mode for the peroxide adduct of T1Hg Lc is as a μ-1,1 hydroperoxo, bridging between the type 2 and type 3 coppers (Figure 14A).

Another interesting possibility is to place the peroxo species in the center of the trinuclear cluster and bonded to all three coppers. This structure would utilize all the open coordination positions of all three coppers of the trinuclear cluster. In this alternate structure, the OH bridge between the two coppers has to be removed. This is because single-atom dibridged coppers cannot be at a distance greater than 3.1 Å, as at this distance, the two oxygen atoms of the bridges would be closer than their van der Waals radii. From the EXAFS data, a Cu···Cu distance at 3.4 Å (and none at 3.1 Å) is observed. Hence the hydroxide bridge between the type 3 coppers would have to be eliminated with the peroxo ligand binding in a μ_3 $(\eta^1)_3$ mode in the center of the trinuclear cluster. Recently, a tetrameric cupric peroxo complex with a μ_4 $(\eta^1)_4$ binding mode has been structurally characterized.[76] The integrated intensity of the peroxo−Cu CT bands in the adduct and intermediate (Figure 13A) are higher than that of the hydroperoxo model (Figure 13D) but is consistent with this μ_3 $(\eta^1)_3$ binding mode. In this binding mode, the hydroxide bridge between the type 3 coppers in the fully oxidized, resting trinuclear site would be dioxygen derived. This alternate possible binding mode is given in Figure 14B. It should be noted that the EXAFS data analysis cannot distinguish between models A and B. However, further experiments to distinguish between the two possible binding modes given in Figure 14A,B are underway.

The two possible bridging modes of peroxide binding to the trinuclear Cu cluster site are different from that proposed for the H_2O_2 adduct of AO based on crystallography.[21] In this peroxide adduct structure, peroxide binds terminally to one of the type 3 coppers, all bridging is eliminated, and the distances between the coppers in the trinuclear cluster are 4.8, 4.5, and 3.7 Å.[21] This structure is not appropriate for the peroxide adduct of T1Hg Lc in solution. Only one paramagnetic copper in the adduct exists, and no new signals are observed even at very high powers in the He EPR or in the LT MCD spectra, indicating the absence of any additional unbridged paramagnetic coppers. Also a strong outer shell Cu···Cu peak at 3.4 Å is seen from the FT of the EXAFS data which is significantly shorter than the smallest distance between the coppers in the AO−H_2O_2 crystal structure. Such a distinctive feature requires a small pairwise Debye−Waller factor, hence a bridging ligand having a strong bonding interaction between the two coppers. The same T1Hg Lc peroxide adduct structure is present in the native enzyme, at room and low temperatures and at low (5) and high (8) pHs. Our preliminary results of H_2O_2 binding to AO in solution suggest that the difference between the peroxide adduct of AO crystals and Lc in solution may relate to the lower binding constant of H_2O_2 to AO ($\leq$0.5 M^{-1}) and the instability of AO toward reaction with H_2O_2.[77] A 50% depletion of the Cu site to which the peroxide is bound is observed in the crystal structure of the AO−peroxide adduct[21] consistent with the reduced stability of AO toward H_2O_2.

This study has demonstrated that the peroxide adduct and the peroxy intermediate are structurally similar. Since the peroxide intermediate has the same kinetic rate of formation as the "native intermediate" [27] and decays to this form,[32] understanding the geometric and electronic structure of the peroxide level intermediate is key to understanding the catalytic mechanism of O_2 reduction on a molecular level. The structural models of bridging between the type 2 and type 3 (Figure 14A,B) provide insight into the catalytic reduction of O_2 to H_2O. First, it is clear why the type 2 copper is required for the reduction of O_2 since bridging to this center is involved in stabilization of the peroxide intermediate. The geometric structure of bridging to the type 3 site would facilitate the first two-electron transfer to the bound O_2 to form the peroxide level oxygen intermediate. The geometry of bridging between the type 2 and type 3 sites in the trinuclear site of the multicopper oxidase is different from the side-on binding mode in the binuclear site of Hc and Tyr.[15,52] This correlates with the difference in function of reduction of O_2 to H_2O in the

(70) Karlin, K. D.; Ghosh, P.; Cruse, R. W.; Farooq, A.; Gultneh, Y.; Jacobson, R. R.; Blackburn, N. J.; Strange, R. W.; Zubieta, J. *J. Am. Chem. Soc.* **1988**, *110*, 6769.
(71) Ross, P. K.; Solomon, E. I. *J. Am. Chem. Soc.* **1990**, *112*, 5871.
(72) Cole, A. P.; Root, D. E.; Mukherjee, P.; Solomon, E. I.; Stack, T. D. P. *Science* **1996**, *273*, 1848.
(73) Ghosh, P.; Tyeklar, Z.; Karlin, K. D.; Jacobson, R. R.; Zubieta, J. *J. Am. Chem. Soc.* **1987**, *109*, 6889.
(74) Mahroof-Tahir, M. Ph.D. Thesis, Johns Hopkins University, 1992.
(75) Mahroof-Tahir, M.; Murthy, N. N.; Karlin, K. D.; Blackburn, N. J.; Shaikh, S. N.; Zubieta, J. *Inorg. Chem.* **1992**, *31*, 3001.
(76) Reim, J.; Krebs, B. *Angew. Chem., Int. Ed. Engl.* **1994**, *33*, 1969.
(77) Sundaram, U. M.; Palmer, A. E.; Solomon, E. I. Unpublished results.

multicopper oxidases vs reversible binding and activation of O_2 in Hc and Tyr, respectively.

Reduction of O_2 by laccase appears to occur in two $2e^-$ steps. The first is rate determining. This type 2/type 3 bridging mode for the first $2e^-$-reduced, peroxide-level intermediate would facilitate the second $2e^-$ reduction (from the type 2 and type 1 centers) in that the peroxide is directly coordinated to a reduced type 2 copper, and the reduced type 1 is coupled to the type 3 by the covalent Cys-His linkage.[78] Such a $2e^-$ transfer to the peroxide is required by the large Franck−Condon barrier associated with breaking the O−O bond, which requires a large thermodynamic driving force for the rapid reduction of peroxide.[32,79] This second $2e^-$ reduction produces the "native intermediate" which from MCD studies is best described as a Cu(II) trimer with an additional hydroxide bridge between the type 2 and type 3 centers.[27] This could decay to the resting enzyme with a hydroxide derived from O_2 terminally bound to the type 2 center as is observed from $^{17}O_2$ labeling studies.[24,25] Studies are underway to describe in greater detail the geometric and electronic structure of the "native intermediate" and to understand the factors involved in the decay of the peroxy and native intermediates.

(78) Lowery, M. D.; Guckert, J. A.; Gebhard, M. S.; Solomon, E. I. *J. Am. Chem. Soc.* **1993**, *115*, 3012.

(79) Sawyer, D. T. *Oxygen Chemistry*; Oxford University Press: New York, 1991.

Acknowledgment. We are grateful to the National Institutes of Health (Grant DK31450 to E.I.S. and RR-01209 to K.O.H.) and the National Science Foundation (Grant CHE-9423181 to K.O.H.) for support of this work. The SSRL is supported by the Department of Energy, Office of Basic Energy Sciences, Divisions of Chemical and Material Sciences, and in part by the NIH, National Center for Research Resources, Biomedical Technology Program, and by DOE's Office of Health and Environmental Research. We gratefully acknowledge Ms. Laurie Addleman's contribution to the T2D experiments and Research Corp. (Grant HS0429) for funding her research. The computing facilities of the Stanford Department of Chemistry is supported, in part, by a grant from the NSF (CHE-9408185).

Supporting Information Available: Absorption spectra of H_2O_2 reaction with T1Hg Lc at low temperature, absorption and EPR spectra of H_2O_2 reaction with native Lc and absorption, EPR and CD spectra of H_2O_2 reaction with T2D Lc, EPR power saturation behavior at He temperatures of resting and peroxide adduct T1Hg Lc, and Gaussian resolved MCD, absorption, and CD spectra in the ligand field region (5 pages). See any current masthead page for ordering and Internet access instructions.

JA972039I